EES Batteries

REVIEW

View Article Online
View Journal | View Issue

Cite this: *EES Batteries*, 2025, **1**, 1371

Insights into solvent molecule design for advanced electrolytes in lithium metal batteries

Xiao Zhu and Xiaoli Dong *

Received 16th September 2025,
Accepted 22nd September 2025

DOI: 10.1039/d5eb00174a

rsc.li/EESBatteries

Lithium metal batteries have attracted significant attention due to their promising high energy density. However, inherent limitations of lithium metal anodes, such as high reactivity, lithium dendrite growth, and the formation of "dead Li", restrict their practical application. Electrolyte engineering can significantly enhance the performance of lithium metal batteries by optimizing the solvation structure, wherein the solvent molecules play a crucial role in determining the intrinsic physicochemical properties of the electrolytes. Through rational molecular structure optimization, the performance of the electrolyte can be intrinsically enhanced, and its formulation can be substantially improved. Herein, a comprehensive and in-depth summarization of recent advances in the design of electrolyte solvents for lithium metal batteries is presented, along with a critical evaluation of the strengths and limitations of various solvent molecules, including esters, ethers, and other solvent molecules containing heteroatoms. Additionally, an overview of fundamental molecular design principles has been distilled to effectively guide the exploitation of new solvents.

Broader context

The extremely high theoretical specific capacity and low redox potential have spurred the rapid development of the lithium metal anode. Nevertheless, its high reactivity makes it prone to undergoing side reactions with organic electrolytes, significantly degrading the cycle life of lithium metal batteries. Moreover, the non-uniform lithium deposition triggers the uncontrollable growth of lithium dendrites and the formation of "dead Li", both of which introduce serious safety hazards. Electrolyte engineering, particularly solvent design, can tune solvation structures and interfacial properties to address these issues. Through rational molecular structure design, a variety of solvents with distinctive properties have been developed. This review systematically summarizes the distinct structural features of various types of solvents, including esters, ethers, and other solvent molecules containing heteroatoms (N, S, P, Si), along with their applications in the electrolytes of lithium metal batteries, aiming to provide an overview of molecular design principles and guide the future exploitation of new solvent molecules.

1. Introduction

Owing to their high energy density, long cycle life, environmental friendliness, and potential for flexible modular design, lithium-ion batteries (LIBs) have progressively permeated various aspects of our daily lives and become an indispensable tool over the past few decades.[1,2] In recent years, the LIB industry has experienced rapid growth alongside the rise of electric vehicles, striving to fulfill the commercial demands for fast charging, extended endurance, reduced weight, and wide temperature adaptability.[3,4] However, the theoretical specific capacity of current commercialized anode materials, such as graphite (372 mAh g^{-1}), remains relatively low.[5] This greatly restricts the energy density of LIBs to satisfy the mileage requirements of new energy vehicles, presenting a significant gap compared with the traditional fuel vehicles.[6] Therefore, there is a critical need to develop novel anode materials. Lithium metal anode (LMA) has garnered significant attention due to its exceptionally high theoretical specific capacity (3860 mAh g^{-1}) and low redox potential (−3.04 V *vs.* standard hydrogen electrode).[7,8] Theoretically, when paired with appropriate lithium-containing transition metal oxide cathodes, the energy density of lithium metal batteries (LMBs) could achieve >500 Wh kg^{-1}, significantly surpassing that of current LIBs (100–300 Wh kg^{-1}).[9] In addition, the abundant supply of Li from LMA enables the full utilization of Li-free cathodes that rely on multi-electron reactions, such as Li-sulfur batteries and Li-air batteries, thereby further enhancing the energy density.[10,11]

Nonetheless, the development of LMBs is impeded by several critical scientific challenges. Highly reactive lithium

Department of Chemistry and Shanghai Key Laboratory of Molecular Catalysis and Innovative Materials, Institute of New Energy, iChEM (Collaborative Innovation Center of Chemistry for Energy Materials), Fudan University, Shanghai 200433, China. E-mail: xldong@fudan.edu.cn

metal is susceptible to side reactions with organic electrolyte solvents like carbonates, leading to reduced plating/stripping coulombic efficiency (CE), as well as a shortened battery cycle life.[12,13] During the cycling process of LMBs, uneven lithium deposition may result in uncontrolled growth of Li dendrites, accompanied by significant volume expansion.[14,15] This will lead to the pulverization of LMA and the formation of electrically inactivated "dead Li", which will further accelerate the side reactions and degrade the CE.[16] Additionally, the formation of Li dendrites not only leads to the rupture of the solid–electrolyte interphase (SEI) and results in poor cycling stability of LMBs, but can also penetrate the separator, causing the battery to short circuit. This issue is particularly concerning when flammable ether or ester-based electrolytes are employed, as it significantly increases the safety risk.[17] Thus, it is imperative to develop effective strategies to inhibit the growth of lithium dendrites and achieve highly reversible lithium metal plating/stripping, which are critical for constructing high-energy-density LMBs.

As an essential component of LMBs, the electrolyte plays an indispensable and pivotal role, not only serving as a medium for ion transport, but also significantly influencing the operating temperature range, safety performance, and cycling stability of LMBs. Numerous research studies have demonstrated that the solvation structure of Li^+ in the electrolyte is intimately related to the formation of the SEI.[18] Hence, through meticulous electrolyte design, the deposition behavior of lithium metal and the interfacial chemistry can be precisely regulated, which is essential for conquering the limitations of LMBs and enhancing the electrochemical performance. Currently, a variety of electrolyte modification strategies have been developed to modulate the solvent structure, especially the Li^+ primary solvation shell, or regulate the SEI, including high/localized high-concentration electrolytes (HCEs/LHCEs),[19] high-entropy electrolytes (HEEs),[20] weak-solvating electrolytes (WSEs),[21] liquefied gas electrolytes,[22] the introduction of additives,[23] and molecular design of novel lithium salts and solvents.[24] Among these approaches, designing new solvent molecules offers a fundamental improvement in the physicochemical properties of electrolytes from a chemical standpoint, transcending the inherent limitations of conventional solvent molecules and achieving essential optimization for LMBs.[25] Moreover, rational molecular design does not require the introduction of multiple components to create complex electrolyte formulas compared with other methods, which thus emerges as a promising strategy for practical LMBs. Considering the compatibility with LMA and the prospects for practical applications, the design of solvent molecules typically needs to satisfy the following criteria: (1) having excellent reductive stability and being resistant to side reactions with lithium metal; (2) possessing adequate solubility to effectively dissolve lithium salts and enabling a rapid desolvation process to optimize the surface dynamic evolution; (3) exhibiting favorable oxidative stability to ensure compatibility with commercial cathodes; (4) endowed with a relatively wide liquid temperature range to accommodate usage under extreme conditions; (5) having a convenient and cost-effective synthetic preparation process; (6) having a high flash point and being non-flammable to ensure safety (Fig. 1). Furthermore, the desolvation process of Li^+ during the charging and discharging processes critically affects the kinetic behavior of batteries, particularly under low-temperature conditions. As temperature decreases, the desolvation process and the ion movement across the SEI significantly slows down, leading to increased polarization and a reduction in the achieved capacity. Therefore, the desolvation process must be considered in the molecular design of solvents. By implementing rational structural modifications—such as modulating steric hindrance and fine-tuning coordination ability—the solvent can maintain a sufficiently high dielectric constant and donor number (DN) to ensure effective lithium salt dissolution, while concurrently reducing coordination strength to facilitate faster desolvation kinetics. Advanced *in situ* characterization techniques offer valuable tools for investigating the desolvation process. Specifically, *in situ* infrared spectroscopy can be employed to monitor dynamic changes in the solvation structure of interfacial electrolytes during desolvation, while *in situ* MRI can track variations in interfacial anions throughout the process. These approaches collectively provide critical insights that guide the rational selection of solvent molecules.[26]

A thorough and in-depth comprehension of the design principles governing solvent molecules is crucial for advancing the field of electrolyte engineering. Despite numerous outstanding works that have been reported, primarily centering on the macroscopic and holistic design of the electrolytes, a detailed review dedicated to research progress in solvent molecule innovation remains absent. Herein, this review focuses on novel solvent molecule design in recent years, systematically summarizing the distinct structural characteristics of various types of solvents, including esters, ethers, and other solvent

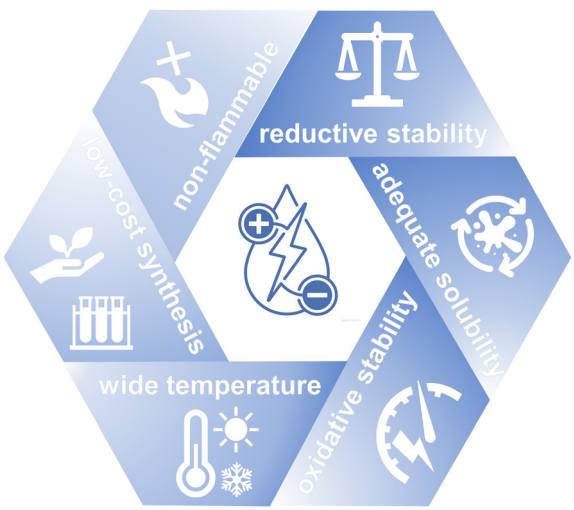

Fig. 1 Illustration of the design criteria for the solvent molecule in LMB electrolytes.

molecules containing heteroatoms (N, S, P, Si), as well as their applications in the electrolytes of LMBs. In addition, an overview of molecular design principles has been summarized, with the objective of guiding the exploitation of new solvents for LMBs in the future.

2. Ester solvents

As the predominant electrolyte solvents in commercial LIBs, ester solvents, particularly the carbonates such as ethylene carbonate (EC), dimethyl carbonate (DMC), diethyl carbonate (DEC), and ethyl methyl carbonate (EMC), exhibit superior oxidative stability and demonstrate exceptional overall performance in LIBs.[27] In addition, esters exhibit a relatively low melting point and flash point, consequently demonstrating reduced flammability.[28] However, owing to the strong conjugated electron-withdrawing effect of the carbonyl oxygen in esters, the carbonyl carbon exhibits an electropositive character, which make esters susceptible to gaining electrons from the external environment and undergoing reductive reactions, resulting in poor reductive stability. Therefore, when ester solvents are applied to LMA that exhibit high reductive activity, continuous side reactions will occur, leading to the formation of an uneven, unstable, and mechanically fragile SEI dominated by organic components.[29] Such SEI will result in an uneven distribution of Li^+ flux, which could subsequently lead to the formation of detrimental Li dendrites and exacerbate side reactions, thereby establishing a vicious cycle.[30,31] Hence, for the modification of ester solvents, it is essential to improve the reductive stability or construct a stable SEI to prevent side reactions and dendrite growth by molecular design. On the one hand, the introduction of electron-donating groups could reduce the electropositivity of the carbonyl carbon; on the other hand, substitution of fluorine atoms could promote the formation of a robust LiF-rich SEI with high ionic conductivity.[32] In this section, a comprehensive summary of the recent advancements in ester solvents design will be proposed.

2.1. Carbonate solvents

Depending on the structure, carbonates can be classified into two types: linear carbonates and cyclic carbonates. The former demonstrates weaker orientational polarization and low viscosities, resulting in a superior desolvation ability and high lithium-ion transport in the electrolyte, whereas the latter exhibit a higher dielectric constant and predominantly occupy the inner layer of the solvation shell, participating in the formation of a stable SEI through ring-opening reactions.[33] Therefore, commercial electrolytes for LIBs typically consist of mixed linear and cyclic carbonates. For LMA, integrating the structural characteristics of the two types of carbonates into a single molecule is expected to achieve enhanced reductive stability compared with physical mixing. Through the transesterification reaction between DMC and the ring-opening product of EC, a novel carbonate solvent dimethyl 2,5-dioxahexanedioate (DMDOHD) can be obtained, which structurally incorporates the features of EC and DMC, and also shares similar structural features with other linear carbonates like EMC (Fig. 2a).[34] The structural similarity endows DMDOHD with favorable SEI-forming capability, enhanced desolvation performance, and remarkable oxidative stability. Based on this, 1 M-$LiPF_6$-DMDOHD electrolyte demonstrates excellent high-voltage tolerance, maintaining stability at 5.2 V in the potentiostatic floating test (Fig. 2b). When adopted in Li||$LiNi_{0.5}Mn_{1.5}O_4$ (LNMO) full cells, the electrolyte exhibits exceptional cycling stability, maintaining a high capacity retention of 94% after 200 cycles at C/5. Similarly, another linear carbonate bis(2-methoxyethyl) carbonate (BMC) can also be synthesized *via* intramolecular hybridization by introducing ether functional groups onto DMC, making BMC endowed with combined advantages of both esters and ethers (Fig. 2c).[35] As an electron-donating group, the introduced alkoxy reduces the electropositivity of the carbonyl carbon and enhances the reductive stability, thereby ensuring that the BMC-based electrolyte demonstrates impressive Li plating/stripping CE of 99.4%. Simultaneously, BMC still maintains excellent oxidation stability, enabling the high-loading Li||$LiNi_{0.8}Co_{0.1}Mn_{0.1}O_2$ (NCM811) battery to retain 92% of its initial capacity after 150 cycles. These two molecules have elongated their molecular chains through the incorporation of functional groups, thereby enhancing steric hindrance and intermolecular interactions. Consequently, DMDOHD and BMC exhibit partly reduced solvation tendencies and higher flash and boiling points compared with traditional carbonates, which invest the relevant electrolytes with excellent electrochemical performance and high safety. Nonetheless, this molecular design approach typically involves a complex synthesis process and restricts the molecular structure to long-chain linear carbonates, thereby limiting its applicability to a narrower range of structural variations.

Compared with the hybridization of different functional groups, fluorination is a more prevalent strategy in molecular structure design. In the presence of a reducing agent like Li, fluorinated molecules undergo defluorination to form corresponding fluorides, facilitating the formation of a LiF-rich SEI on the surface of LMA.[32] LiF exhibits high interfacial energy and mechanical strength, which can induce rapid and uniform nucleation of Li^+, inhibit the growth of lithium dendrites, and ensure the long-term stable cycling of LMA.[36] In addition, the intermolecular interactions in fluorinated solvents are weaker due to the lower polarizability of F, resulting in alleviated desolvation barrier of Li^+ and facilitating homogeneous deposition of Li.[37] Moreover, the exceptionally high bond energy of the C–F bond typically confers superior chemical and thermal stability to fluorinated solvents.[38] Therefore, fluorination is anticipated to address the inherent instability of carbonates with LMA. By introducing fluorine at varying positions and in different quantities on common carbonate molecules, a diverse range of fluorinated carbonate solvents have been designed for LMBs. Among these, fluoroethylene carbonate (FEC), derived from the fluorination of EC, is the most representative solvent, which not only facilitates the for-

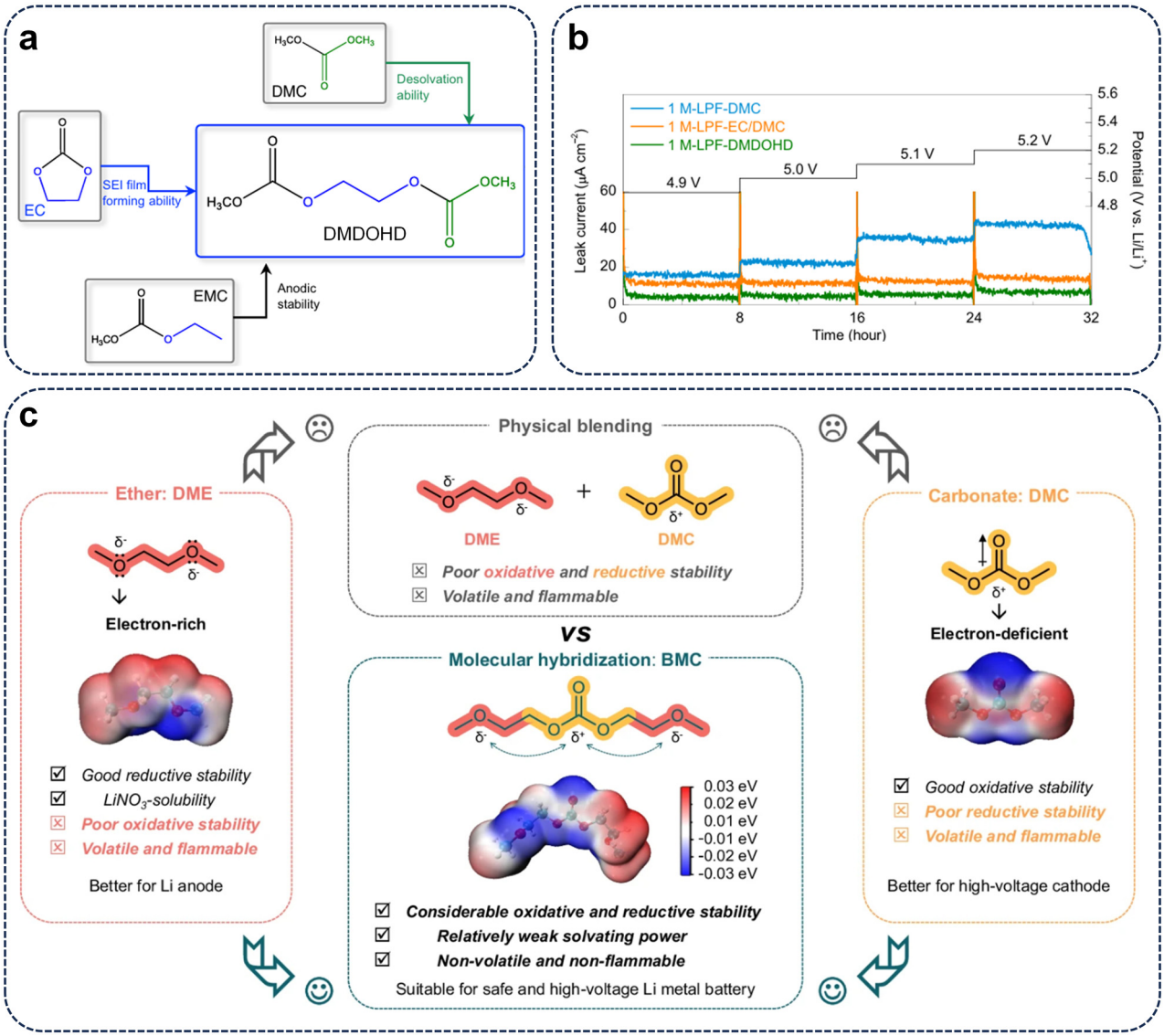

Fig. 2 (a) Design rationale of DMDOHD. (b) Potentiostatic floating profiles of Li||LNMO cells with various carbonate-based electrolytes. Reproduced with permission.[34] Copyright 2024, Springer Nature. (c) Schematic illustration of BMC molecule design. Reproduced with permission.[35] Copyright 2024, Springer Nature.

mation of a stable SEI, but also enhances the stability of the Li plating/stripping process under higher current densities and capacities.[39] Hence, FEC has been extensively utilized as an efficient film-forming additive in various advanced electrolyte systems, and is commonly employed as a co-solvent to improve the electrolyte compatibility with LMA.[40,41] By further fluorination of FEC, the resultant difluoroethylene carbonate (DFEC) exhibits a lower lowest unoccupied molecular orbital (LUMO) energy level compared with FEC (Fig. 3a), consequently facilitating easier defluorination and promoting the formation of a more stable SEI layer enriched with LiF.[42] In addition, the increased degree of fluorine substitution further enhances the oxidative stability. The Li||$LiNi_{0.6}Co_{0.2}Mn_{0.2}O_2$ (NCM622) battery utilizing DFEC as SEI enabler in the electrolyte could demonstrate a capacity retention exceeding 82% after 400 cycles and an average CE of 99.95%, surpassing the battery using FEC.[43] Nevertheless, owing to the intrinsic instability of cyclic carbonates, which are susceptible to ring-opening decomposition, as well as the defluorination reaction of fluorine atoms, cyclic fluorinated carbonates are typically limited to use as a minor cosolvent/additive (<30%) in electrolytes and are unsuitable as the primary solvent.

In contrast, linear fluorinated carbonates exhibit better stability, making them more suitable as the primary solvent. By perfluorinating both terminal ethoxy groups of the DEC molecule, the binding between Li^+ and the solvent is weakened, which facilitates the desolvation of Li^+ and significantly reduces the electrical resistance during the electrochemical process. Simultaneously, full-fluorination further enhances the oxidative stability. Hence, the obtained bis

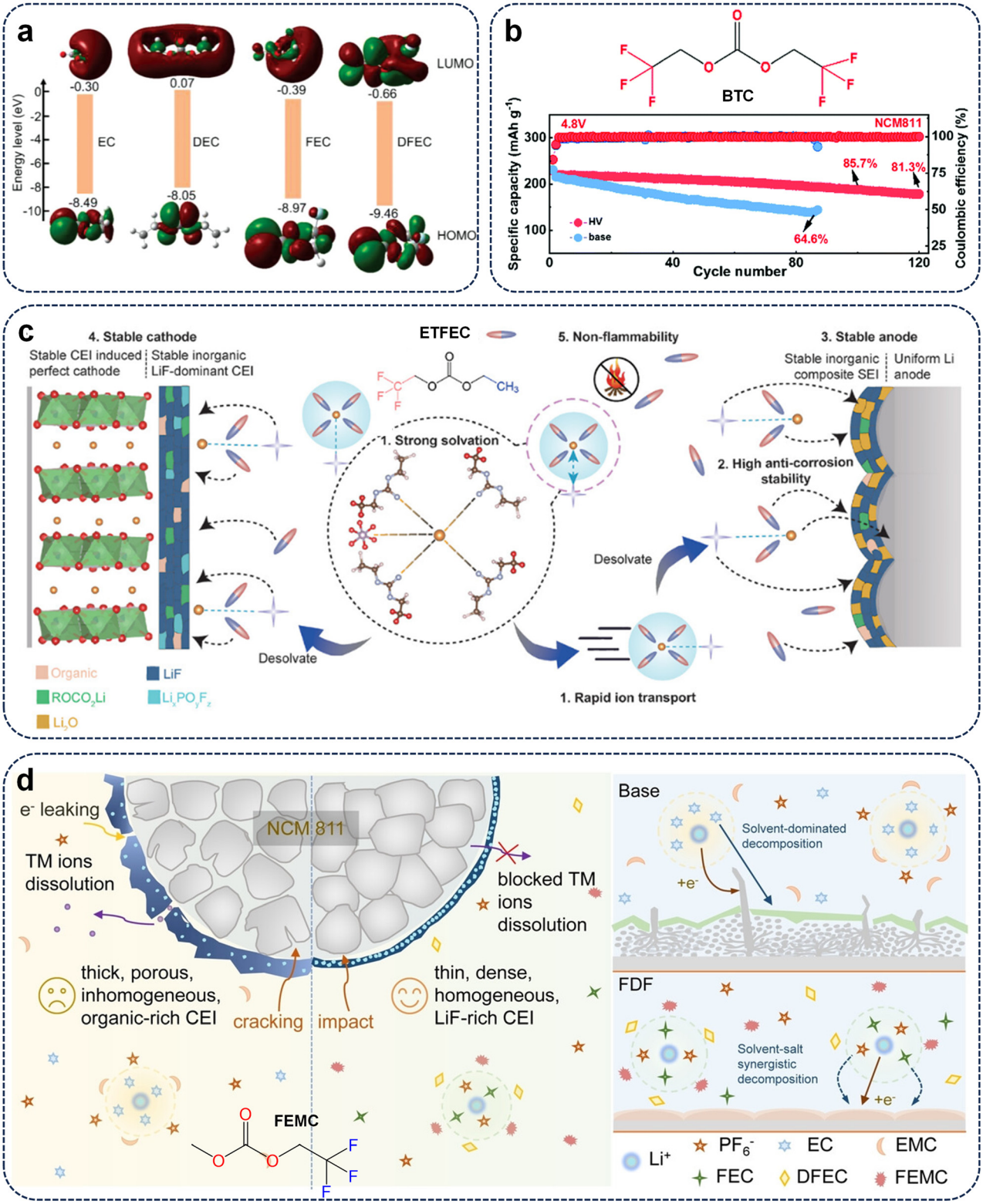

Fig. 3 (a) Schematic of LUMO/HOMO energies of EC, DEC, FEC, and DFEC. Reproduced with permission.[42] Copyright 2021, Wiley-VCH. (b) Structural diagram of BTC and the cycling performance of Li||NCM811 cells using BTC-based electrolyte (nominated as HV) with a cut-off voltage of 4.8 V. Reproduced with permission.[44] Copyright 2022, The Royal Society of Chemistry. (c) Overall evaluation of the asymmetric ETFEC-based electrolyte. Reproduced with permission.[45] Copyright 2024, Wiley-VCH. (d) Schematic illustration of the roles played by the FEMC-based electrolyte (nominated as FDF) in stabilizing the high-voltage NCM811 cathode and the SEI formation process. Reproduced with permission.[48] Copyright 2024, Wiley-VCH.

(2,2,2-trifluoroethyl) carbonate (BTC) solvent exhibits excellent thermal stability over a wide operating temperature range from −30 to 70 °C and demonstrates stable cycling performance in Li||NCM811 cells at an ultrahigh cut-off voltage of 4.8 V for more than 100 cycles (Fig. 3b).[44] Nevertheless, despite the significant enhancement in oxidative stability of the solvents achieved through this symmetrical perfluorination strategy, its overall LMB performance remains suboptimal. Perfluorinated solvents demonstrate a non-polar character and low polarizabilities, resulting in weak solvation ability and low ionic conductivity.[32] In contrast, the asymmetrically fluorinated strategy, which combines a highly inert fluorinated structure on one side of the molecule with a solvation-promoting non-fluorinated structure on the other, successfully integrates the high stability of fluorinated carbonates and the strong solvation/ion-conduction advantages of non-fluorinated carbonates while simultaneously addressing their respective limitations.[45] Based on this, the ethyl (2,2,2-trifluoroethyl) carbonate (ETFEC) molecule, which is obtained by fluorination only at one end of the DEC molecule, exhibits remarkably enhanced lithium salt solubility and ionic conductivity (5.52 mS cm^{-1}), significantly surpassing those of the perfluorinated BTC molecule (1.67 mS cm^{-1}) (Fig. 3c). ETFEC can dissolve 5 M lithium bis(fluorosulfonyl) imide (LiFSI) salt and achieve a high Li plating/stripping CE of 99.1%.[46] The EFTEC-based electrolytes, with the further addition of FEC or vinylene carbonate (VC) additives, can enable stable cycling of Li||NCM811 cells for over 200 cycles.[45,47] Similarly, 2,2,2-trifluoroethyl methyl carbonate (FEMC), which is derived from the fluorination of the ethoxy terminus of the EMC molecule, also demonstrates excellent performance. By incorporating minor amounts of FEC and DFEC additives, the FEMC-based electrolyte can facilitate the formation of a SEI layer enriched with LiF and Li_2O on LMA through the synergistic decomposition of the fluorinated solvents and PF_6^- anions, facilitating smooth lithium metal deposition. It can also form a stable cathode–electrolyte interphase (CEI) on the cathode surface, thus enabling a pioneering 4.8 V-class lithium metal pouch cell with an energy density of 462.2 Wh kg^{-1} to cycle stably for 110 cycles under harsh conditions.[48] Further introducing boron-containing additives, the FEMC-based electrolyte can acquire fire-extinguishing properties, while effectively inhibiting the transition metal dissolution and the gas production on the cathode side.[49] In addition, through the synergistic effect of multiple components, the FEMC-based electrolyte exhibits extraordinary temperature adaptability from −85 to 70 °C.[50] Although these fluorinated carbonate solvents have demonstrated some success, their application is limited by relatively poor reductive stability, making them unsuitable as standalone solvents, and they need to be used in conjunction with co-solvents or additives. Furthermore, the fluorine substitution strategy primarily emphasizes perfluorination at the termini of the molecular chains. The design involving partial fluorination at other positions remains underdeveloped.

2.2. Carboxylate solvents

Compared with carbonate solvents, carboxylate solvents possess a lower melting point and viscosity, thereby imparting the electrolyte with an extended liquid temperature range and enhanced ionic conductivity.[51] In the carboxylate molecules, the unbonded electrons of the carbonyl oxygen are partially delocalized through conjugation with the adjacent ester oxygen, thus reducing the electron cloud density around the carbonyl oxygen. This effect weakens the binding energy between the carboxylate solvent and Li^+, leading to a more rapid desolvation process. In the carbonate molecules, due to the presence of an additional ester oxygen that provides an electron donation effect, the unbonded electrons are less affected by the conjugation effect and are more localized. Therefore, carboxylate solvents are better suited for low-temperature applications owing to the improved electrochemical kinetics.[52] Generally, the short-chain carboxylates, such as methyl acetate (MA) and ethyl acetate (EA), exhibit relatively low viscosities, thereby minimizing viscous resistance to ionic transport. However, the SEI films generated from them are insufficiently robust to inhibit continuous side reactions of the electrolyte. In contrast, long-chain carboxylates, such as ethyl propionate (EP) and ethyl butyrate (EB), facilitate the formation of a protective interface.[53] Nevertheless, similar to carbonates, carboxylates also show poor compatibility with LMA in general, along with inferior oxidative stability due to the more localized unbonded electrons.[54] Consequently, unmodified carboxylates are not appropriate as the primary solvents in LMBs, unless they are utilized as additives or in LHCEs.[55–57]

Similarly, in fluorinated carboxylate solvents, the introduction of F optimizes the interfacial layer on the LMA surface, improving the compatibility of fluorinated carboxylate-based electrolytes with LMBs. Meanwhile, the electron-withdrawing effect of the fluorine atoms further reduces the binding affinity between the fluorinated carboxylate molecule and Li^+, thereby accelerating the desolvation kinetics at low temperature. Therefore, the fluorinated carboxylate solvents demonstrate superior adaptability in low-temperature LMBs. Compared with the alkoxy side, fluorination on the acyl side exhibits a more pronounced electron-withdrawing effect, which is attributed to the oxygen atom on the alkoxy side having a shielding effect on the $–CF_n$ group. Hence, through the fluorination on the acyl side, numerous fluorinated carboxylate molecules, such as methyl trifluoroacetate (MTFA),[58] methyl 3,3,3-trifluoropropionate (MTFP),[59,60] and ethyl 4,4,4-trifluorobutyrate (ETFB),[61,62] have been designed and applied in the electrolytes of low-temperature LMBs. Owing to the relatively low LUMO energy levels, these fluorinated carboxylated-based electrolytes promote the formation of a LiF-rich SEI, which can maintain high ionic conductivity and structural stability at low temperatures, thus significantly reducing interfacial resistance. Since the diffusion of Li^+ through SEI at low temperature is the most critical factor that limits the battery performance, these electrolytes have substantially improved the low-temperature performance of LMBs.[58] When the electro-

lyte formulation is further optimized, these carboxylate-based electrolytes can be adapted for battery operation under more stringent conditions. By implementing the LHCE strategy, the ethyl trifluoroacetate (ETFA)-based electrolyte can endure a high voltage up to 5 V, enabling stable cycling of the Li||LNMO battery for 300 cycles with a cutoff voltage of 4.95 V.[63] Assisted by readily dissociated lithium salts, $LiBF_4$ and lithium difluoro (oxalato) borate (LiDFOB), the ethyl 3,3,3-trifluoropropanoate (ETFP)-based electrolyte delivers a high energy of 442.5 Wh kg^{-1} with 80% capacity retention after 100 cycles in industrial anode-free pouch cells under harsh testing conditions.[64] Compared with perfluorinated carboxylates, reducing the number of fluorine atoms improves both ionic conductivity and salt dissociation ability due to the enhanced polarity. Notably, moderately fluorinated carboxylates ($-CHF_2$) strike an optimal balance between weak affinity and elevated ionic conductivity.[52] However, the reduction in fluorination degree impedes the desolvation process at low temperature and hinders the formation of stable interfaces, consequently restricting the performance of less-fluorinated carboxylate-based electrolytes in LMBs.[65,66] Overall, fluorinated carboxylates encounter similar challenges to carbonates. Their inadequate reductive stability limits their use as standalone solvents, necessitating the addition of film-forming additives such as FEC. Hence, the development of novel carboxylate solvents has been relatively limited.

3. Ether solvents

Since ether solvents have no unsaturated groups like carbonyl and possess alkoxyl groups that exhibit strong electron-donating effects, they demonstrate exceptionally high reductive stability. Therefore, ether solvents exhibit superior compatibility with LMAs compared with ester solvents.[67,68] The low viscosity and high ionic conductivity of ether solvents facilitate rapid Li^+ transport and efficient interfacial charge transfer, while their low freezing points ensure superior battery performance at sub-zero temperatures.[69] Additionally, ether solvents can effectively dissolve sufficient $LiNO_3$, which is an essential additive for stabilizing the Li interface and has been extensively utilized in the electrolytes of LMBs.[70,71] By modulating the number and positions of oxygen atoms, as well as the lengths of carbon chains in linear ethers, a diverse array of ether solvent structures has been systematically designed. Among these, the most successful commercialization achievements are 1,2-dimethoxyethane (DME) and 1,3-dioxolane (DOL), which have been widely applied in constructing the electrolytes for LMBs or lithium–sulfur batteries due to their extraordinary reductive stability and high lithium salt solubility.[72,73] However, along with the high reductive stability, ether solvents also exhibit poor oxidative stability. Due to the presence of unbonded electrons on the ether oxygen atom, ether solvents exhibit strong Lewis basicity and are susceptible to electron loss and subsequent oxidation. Consequently, ether solvents are incompatible with common high-voltage cathodes, which restricts their broader development and application.[74] Meanwhile, common linear ethers typically exhibit the structure of ethylene glycol, in which the two oxygen atoms are prone to chelate coordination with Li^+, substantially enhancing the binding energy between the solvent and Li^+. Therefore, ether solvents tend to participate in the solvation structure and subsequent film-forming process, which is detrimental to the formation of anion-derived, inorganic-rich SEI. Furthermore, the high binding energy of ether solvents hinders the desolvation process at the interface, limiting their performance at low temperature.[75] Common strategies involve adjusting the chain length along with the number of oxygen atoms, designing ether molecules with weak solvation ability, and fluorination. In this section, the design strategies and recent research advancements of ether solvents will be reviewed from the perspectives of cyclic and linear ethers.

3.1. Cyclic ether solvents

Cyclic ethers exhibit limited flexibility in forming chelate coordination with Li^+ owing to their rigid structure, endowing them with relatively weak solvation ability. Besides, due to the unique reductive mechanism and interface stabilization effect, various cyclic ether solvents are expected to undergo ring-opening reactions with Li^+, leading to the formation of macromolecular polymeric compounds with excellent flexibility, which consequently enhances the mechanical stability of the interface layer on the LMA.[76] Therefore, DOL is frequently utilized as a co-solvent in conjunction with DME to formulate commercial electrolytes for LMBs. However, due to its strong electron-donating ability, DOL will undergo uncontrollable ring-opening polymerization in the presence of a trace amount of H_2O or Lewis acid like Li^+, leading to electrolyte gelation.[77] By introducing the branched methyl group onto DOL, the reactive sites of the ring-opening reaction can be effectively blocked, along with enhanced steric hindrance of the cyclic structure, thereby inhibiting the ring-opening polymerization of DOL and enabling it to function as a stable single solvent in LMB electrolytes. Based on this, the designed 4-methyl-1,3-dioxolane (4-MDOL) exhibits strong steric hindrance, resulting in reduced solvation capability, which facilitates the accumulation of anions within the inner solvation sheath and promotes the formation of anion-derived interfaces.[78] Hence, the low-concentration (1 M) 4-MDOL-based electrolyte demonstrates excellent electrochemical performance. By leveraging the unique molecular spatial configuration, unforeseen and beneficial effects can also be achieved. 2-Methoxy-1,3-dioxolane (MODOL) can be obtained by introducing a methoxy group as a bridging element at the 2-C position of DOL. Although methoxy is an electron-donating group, the non-bonding hybrid orbitals of the exocyclic oxygen atom partially overlap with those of the endocyclic oxygen atoms due to the unique molecular conformation, which can be taken as a quasi-conjugated effect (Fig. 4a).[79] This results in electron delocalization, leading to the reduction in the electron-donating ability of the oxygen atoms and endowing MODOL with limited solvating power. Hence, the electron-donating methoxy

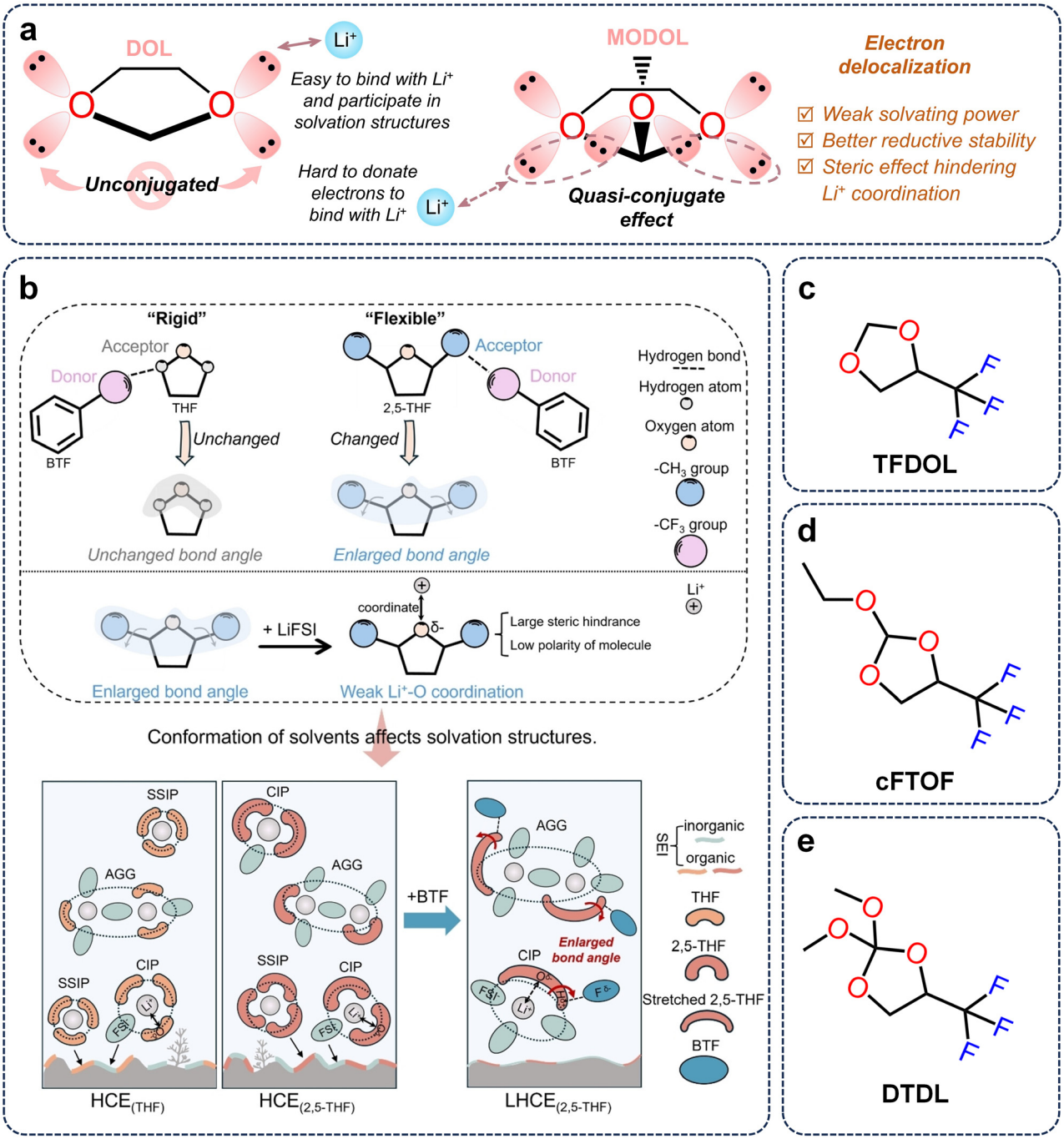

Fig. 4 (a) Schematic illustration of MODOL molecule design. Reproduced with permission.[79] Copyright 2025, Wiley-VCH. (b) Schematics displaying conformational changes of flexible 2,5-THF molecule and the corresponding solvation structure. Reproduced with permission.[83] Copyright 2025, Wiley-VCH. Molecular structure of (c) TFDOL, (d) cFTOF, and (e) DTDL.

exhibits an effect analogous to that of electron-withdrawing groups like fluorine atom, endowing the MODOL-based electrolyte with exceptional cycling stability and wide-temperature performance (−20 to 50 °C). In addition, the methoxy enhances the stability of endocyclic C–O bonds, making MODOL demonstrate higher resistance to decomposition and generate fewer organic SEI components.

Decreasing the number of oxygen atoms, thereby reducing coordination sites, can also realize the weak solvation ability of the cyclic ether solvents. The presence of the single oxygen-contained group of tetrahydrofuran (THF) guarantees it has benign coordination and de-solvation capability with Li^+. Meanwhile, the ultra-low melting point of THF (−108.5 °C) further ensures its electrochemical performance at low temp-

eratures.[80] By incorporating the branched methyl group, 2-methyl tetrahydrofuran (2-MTHF) demonstrates a higher LUMO energy level than THF, indicating enhanced reductive stability.[81] As a highly compatible low-polarity solvent, 2-MTHF can rationally regulate strong Li^+-anion coordination structures, facilitating remarkably high Li plating/stripping CE under rather demanding conditions. However, other research has demonstrated that the interfacial defluorination reaction in THF-based electrolytes with stronger solvation capability proceeds more rapidly, leading to the formation of an amorphous SEI rich in inorganic compounds, which is more effective at inhibiting dendritic lithium growth compared with that formed in 2-MTHF-based electrolyte.[82] Further increasing the number of methyl groups, the resulting 2,5-dimethyl tetrahydrofuran (2,5-THF) solvent has a flexible O–CH–CH_3 chain, the endpoint H atom of which can form strong hydrogen bonds with the F atom of the benzotrifluoride (BTF) diluent. These hydrogen bonds can expand the maximum bond angle within the 2,5-THF molecule, thereby increasing its steric hindrance and decreasing its polarity. Consequently, this leads to an increase in the anion content within the solvation structure, ultimately enhancing the performance of LMBs (Fig. 4b).[83] The assembled Li||sulfurized polyacrylonitrile (SPAN) battery with 2,5-THF-based electrolyte demonstrates impressive stability over 700 cycles with an average CE of 99.8%.

According to experimental and computational studies, the enlarged ring structure of cyclic ethers will weaken the solvating ability.[84] Therefore, the hexatomic cyclic ether, such as 1,3-dioxane (1,3-DX) and 1,4-dioxane (1,4-DX), can facilitate the entry of more anions into the solvation shell, resulting in a lower desolvation energy barrier.[85–87] Compared with DOL, 1,3-DX possesses higher hydrogen-transfer energy, confirming its better antioxidant capacity.[85] Similarly, tetrahydropyran (THP) with a single coordination site is a prototypical weakly solvating solvent that has a cyclic symmetric structure, diminishing the electron density around the O atom in the C–O–C bond.[88] Consequently, THP-based electrolyte exhibits rapid desolvation kinetics, exhibiting superior performance at extremely low temperatures (−50 °C).[89] Moreover, THP can participate in the construction of a deep eutectic electrolyte and demonstrates high temperature tolerance with $LiMn_2O_4$ cathode.[90] In order to further enhance the oxidative stability of the cyclic ether solvents, a series of fluorinated cyclic ethers, such as 4-(trifluoromethyl)-1,3-dioxolane (TFDOL),[91] 2-ethoxy-4-(trifluoromethyl)-1,3-dioxolane (cFTOF),[92] and 2,2-dimethoxy-4-(trifluoromethyl)-1,3-dioxolane (DTDL),[93] has been designed by introducing additional alkoxy or –CF_3 groups (Fig. 4c–e). The introduced electron-withdrawing –CF_3 group lowers the highest occupied molecular orbital (HOMO) energy levels of these molecules and weakens their coordination ability. Among them, cFTOF and DTDL integrate a cyclic fluorinated ether with a linear ether segment to simultaneously achieve high voltage stability and modulate the solvation ability and structure of Li^+. Hence, these fluorinated cyclic ethers can function as a single solvent with low salt concentration (≤2 M), enabling uniform and compact Li deposition and achieving outstanding stability in Li||NCM811 cells. Further increasing the degree of fluorination will substantially decrease the solubility of the cyclic ethers, rendering them incapable of dissolving lithium salts and limiting their functionality to that of diluents.[94–97] Overall, limited by the inherent ring strain, it is challenging to design more novel cyclic ethers with different structures by altering the number of carbon atoms and modifying substitution site.

3.2. Linear ether solvents

As a typical linear ether, DME is widely utilized in the electrolytes of LMBs due to its outstanding reductive stability.[98] However, DME tends to form a stable pentacoordinate complex structure by coordinating with Li^+ *via* the two oxygen atoms within its molecular framework, which endows DME with strong solvation ability, making it dominate the Li^+ primary solvation shells in conventional concentration electrolytes.[99] Such a solvation structure will result in an increased proportion of organic components in the SEI, adversely affecting the Li plating/stripping CE. In addition, DME exhibits relatively inadequate oxidative stability (<4.0 V *vs.* Li^+/Li), which constrains its application in high-voltage LMBs.[100] Therefore, enhancing the performance of DME-based electrolytes commonly necessitates the adoption of the LHCE strategy by increasing the concentration of lithium salt and introducing hydrofluoroether diluents.[101] Attributed to the inherent flexibility of the chain structure in linear ethers, a diverse range of novel solvent molecules with enhanced properties can be systematically designed by modulating the alkyl chain length, incorporating branched chains, or adjusting the number of alkoxy units.

Systematic adjustment of the ether backbone exerts a significant impact on both the Li^+-chelating behavior and the electrochemical stability of the electrolytes. By elongating the length of central carbon chain, 1,3-dimethoxypropane (DMP) can form a six-membered chelate ring with a stronger Li^+-solvation stability compared with DME, which can only form a five-membered chelate ring, effectively suppressing side reactions of labile free solvent molecules on the cathode.[99] Further increasing the number of –CH_2– units in between, the seven-membered chelate ring in 1,4-dimethoxybutane (DMB) exhibits decreased stability, and the ion coordination model shifts from bidentate to monodentate, resulting in reduced oxidative stability (Fig. 5a). In addition, the preferred hydrogen transfer reaction between DMP and anion significantly promotes the accumulation of LiF on the cathode surface, making DMP-based electrolyte demonstrate enhanced performance on Ni-rich cathodes under a high voltage of 4.7 V. However, although this six-membered chelate coordination structure enhances the oxidative stability of the solvent, its strong binding energy with Li^+ is not conducive to its performance at the LMA side, which necessitates increasing the lithium salt concentration to construct a better SEI. Conversely, shortening the length of the central carbon chain can weaken the solvating ability of the ether solvents, leading to an anion-dominant solvation struc-

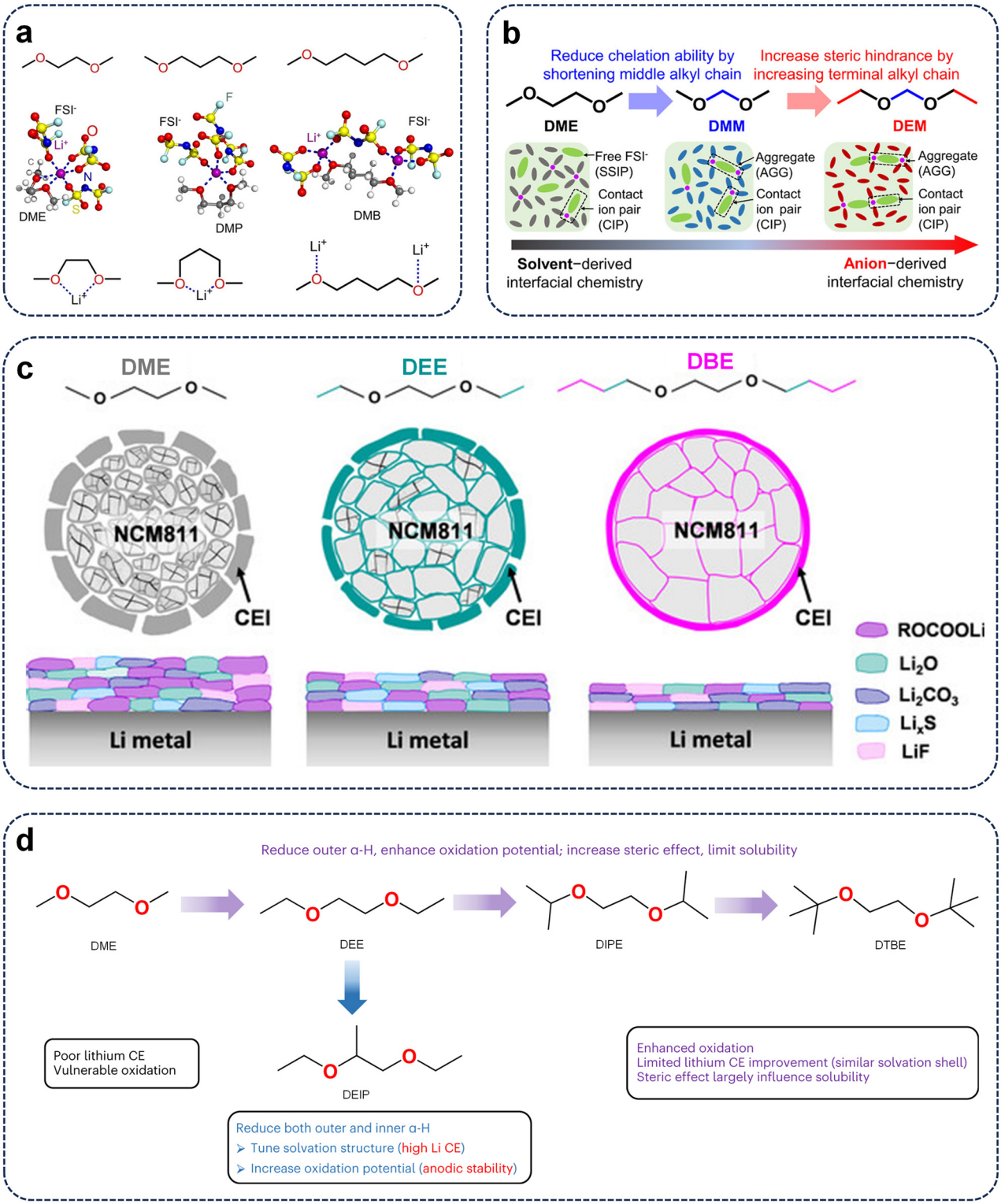

Fig. 5 (a) Molecular structures of DME, DMP, and DMB, along with the corresponding ion-solvation structures. Reproduced with permission.[99] Copyright 2023, Wiley-VCH. (b) Solvent molecular design methodology for DEM. Reproduced with permission.[104] Copyright 2022, American Chemical Society. (c) Molecular structures of DME, DEE, and DBE, and illustration of the effects of them on the interfacial property of NCM811 cathode and LMA. Reproduced with permission.[107] Copyright 2023, Wiley-VCH. (d) Methylation design on DME molecules to introduce branched chains for enhanced steric effects. Reproduced with permission.[109] Copyright 2024, Springer Nature.

ture. By decreasing the number of the central –CH_2– units in DME, the chelate coordination structure is disrupted. The obtained dimethoxymethane (DMM) molecule preferentially adopts the [*gauche*, *gauche*] conformation due to the hyperconjugation effect, resulting in weakened monodentate coordination with Li^+ and lower desolvation energy.[102,103] Further extending the terminal alkyl chain of the DMM molecule could increase the steric hindrance, affording a diethoxymethane (DEM) solvent with ultra-weak solvation ability, which could induce a peculiar solvation structure predominantly composed of contact ion pairs (CIPs) and aggregates (AGGs) when serving as a single solvent with a regular salt concentration (Fig. 5b).[104]

Similarly, extending the terminal alkyl chain of the DME molecule has the same effect of increasing steric hindrance, thereby reducing the solvation ability, while maintaining the chelate coordination structure to ensure adequate solubility.[105] Hence, 1,2-diethoxyethane (DEE) has low dielectric constant and dipole moment, promoting the formation of an inorganic-rich SEI and CEI, thereby demonstrating exceptional low-temperature performance.[106] By further extending the terminal groups of DME from methyl to *n*-butyl, the comprehensive thermodynamic stability of the ether solvent is improved, along with increased boiling/flash point from 84/−2 °C to 203.3/85 °C due to the extended chain length, resulting in the obtained 1,2-dibutoxyethane (DBE) solvent more suitable for high-temperature application. Simultaneously, attributed to the diminished solvation ability, the electrode–electrolyte interactions are suppressed, thereby effectively reducing the catalytic reactivity of NCM811 cathode towards the electrolyte at high voltages and alleviating its surface phase transition and structural degradation (Fig. 5c).[85,107] In addition to modifying the main chain, introducing branched chains to enhance the steric effects can also reduce the solvation power and optimize the solvation structure.[108] Through selective methylation of DME α-H atoms, the molecule's solvation capability, ionic transport, Li^+ desolvation rate and electrochemical stability can be precisely tuned (Fig. 5d).[109] Consequently, the resulting 1,2-diethoxypropane (DEIP)-based electrolyte demonstrates high stability for 150 cycles in 100 mA h Li||$LiNi_{0.8}Co_{0.15}Al_{0.05}O_2$ (NCA) pouch cells, maintaining a high capacity retention of 95%. In addition, the design of an asymmetric structure can also achieve favorable effects, enhancing the performance of a series of asymmetric ether solvents, such as 1-isopropoxy-2-methoxyethane (iPME), 1-butoxy-2-methoxyethane (BME), and 1-isobutoxy-2-methoxyethane (iBME), surpassing that of DME.[110]

In addition to adjusting the alkyl chain, modulating the number of oxygen atoms is another effective approach for ameliorating linear ether solvents. By increasing the number of glycol units and the chain length, a series of glyme ethers with highly solvating power, including diethylene glycol dimethyl ether (G2), triethylene glycol dimethyl ether (G3), and tetraethylene glycol dimethyl ether (G4), demonstrate superior Li^+-binding stability, electro-oxidation resistance, thermal stability, and nonflammability.[111] These glyme ethers can significantly suppress detrimental oxidation side reactions by reducing the lifetime of free labile ether molecules, due to their stronger Li^+ solvating ability.[112] Research demonstrates that longer glyme ethers lead to a more homogeneous SEI, particularly pronounced when used in conjunction with $LiNO_3$, which can minimize surface roughness during Li stripping, and promote compact Li deposits. The homogeneous interfacial properties resulting from higher reductive stability, and slower kinetics due to high desolvation barrier and viscosity, underline stable Li growth in the long glyme ethers.[113] Hence, these glyme ethers possess excellent stability under high voltage and high temperature, expanding the application range of LMBs. By reducing the carbon chain length in the central glycol unit of G3, bis(2-methoxyethoxy)methane (BMEM) solvent with multi-oxygen coordination sites can be obtained, which can coordinate with Li^+ through a bi/tridentate coordination mode. When the BMEM molecule is bent, three oxygen atoms provide a concentrated negative charge to strongly chelate Li^+, generating a novel tridentate coordination, which can effectively maximize the steric hindrance effect due to the competitive equilibrium of three O atoms bonding with Li^+, thereby facilitating the anionic aggregates' formation within the solvation structure (Fig. 6a).[114] Furthermore, certain acetal molecules featuring alkoxyl side chains, such as triethyl orthoformate (TEOF) and trimethyl orthoformate (TMOF), also demonstrate favorable performance attributable to the steric hindrance effect.[115]

Aside from increasing the number of glycol units, reducing the number of oxygen atoms to prevent chelate coordination is another effective strategy to weaken the solvating ability of the ether molecules. Therefore, as a typical monoxy ether, diethyl ether (DE) displays superior weak solvating power, facilitating a rapid desolvation process under ultra-low temperatures (−60 °C).[116] Extending the terminal groups of DE can further reduce the solvation ability while enhancing its oxidative stability (Fig. 6b). Molecular dynamics simulations reveal a reduction in the number of ether molecules within the electrochemical double layer (EDL) of dipropyl ether (DP), which is advantageous for mitigating the direct oxidation of ethers on the cathode surface. Meanwhile, the DP-based electrolyte also preserves the ion aggregation behavior within the EDL, where Li^+ is coordinated by multiple FSI^-. The preferential decomposition of these FSI^- results in the formation of the anion-derived CEI layer. Hence, the reconfiguration of the EDL structure facilitated by the favorable fluidic properties of DP substantially improves the high-voltage performance of the monoxy ethers.[117] Further extending the terminal groups or introducing branched chain, dibutyl ether (DB) and diisopropyl ether (DIP) also exhibit excellent wide-temperature performances.[118,119] Furthermore, owing to the structural simplicity of these monoxy ethers, the incorporation of asymmetric structures can also bring about unforeseen effects. As an asymmetric ether, methyl *n*-butyl ether (MNBE) consists of a lithiophilic oxygen segment at one end and a lithiophobic alkyl chain at the other, exhibiting an amphiphilic structure. In the electrolyte, MNBE will spontaneously form micelle-like structures with Li^+, leading to inert alkyl chains situated in the

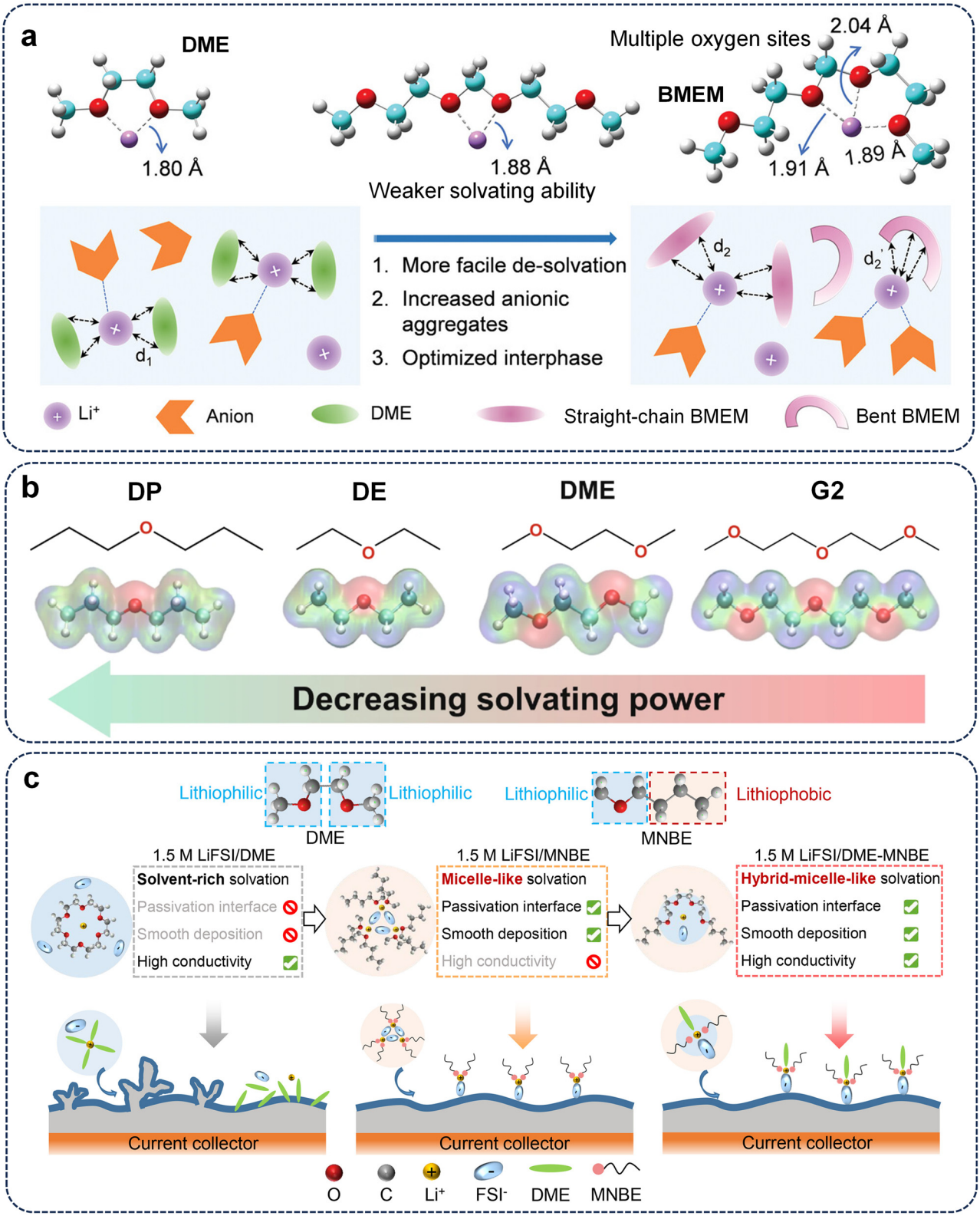

Fig. 6 (a) Optimized binding geometry of Li^+ with DME and BMEM, and illustration of Li^+ solvation structure in DME- and BMEM-based electrolytes. Reproduced with permission.[114] Copyright 2023, Wiley-VCH. (b) The electrostatic potential (ESP) maps of G2, DME, DE, and DP solvents. Reproduced with permission.[117] Copyright 2023, Springer Nature. (c) Construction of micelle-like solvation MNBE-based electrolytes. Reproduced with permission.[120] Copyright 2025, Elsevier.

outer layer of the solvation shell, which can significantly passivate the Li/electrolyte interface due to the lithiophobic feature (Fig. 6c). Introducing MNBE as a co-solvent into 1.5 M LiFSI-DME electrolyte could form a hybrid-micelle-like solvation structure, enabling a high-capacity (7.3 Ah) lithium metal pouch cell to stably cycle for 100 cycles with a high energy density of 503.7 Wh kg^{-1} and a high capacity retention of 84.1%.[120] Similarly, by substituting the straight-chain alkyl group on one side with a bulky cyclopentyl group, cyclopentyl methyl ether (CPME) exhibits reduced coordination ability and an exceptionally low melting point, thereby demonstrating superior low-temperature performance.[121]

Just as in the case of cyclic ether molecules, by leveraging the electron-withdrawing effect of fluorine atoms, the electronegativity of oxygen atoms can be effectively mitigated, thereby reducing the solvation power of linear ethers and enhancing their oxidative stability. By selectively fluorinating the ether molecules, their solvation capabilities can be precisely modulated, enabling the construction of diverse solvation structures. Therefore, numerous fluorinated linear ether solvents have been exploited with outstanding performance. It is worth noting that, owing to the potent electron-withdrawing effect of fluorine atoms, only when the partial fluorination occurs at positions sufficiently distant from the O atom (β-C) can the fluorinated linear ethers preserve the salt-dissolving capability of the electrolytes while inducing the formation of stable SEI.[122,123] The earliest reported fluorinated linear ether, 2,2,3,3-tetrafluoro-1,4-dimethoxylbutane (FDMB), was derived from DMB by introducing fluorine atoms in the central part of the main chain to expand the oxidative window and enhance lithium metal compatibility. Meanwhile, leveraging the stability of the longer alkyl chain, FDMB retains its capability to dissolve lithium salts and conduct lithium ions effectively (Fig. 7a).[29] The FDMB-based electrolyte can construct a solvation structure enriched with AGGs and form a compact ultra-thin SEI (~6 nm) on LMA, thus realizing extremely rapid activation effect in Li||Cu half cells.[124,125] In addition, FDMB can experience favorable defluorination in coordination with both Li^+ and Al^{3+} derived from the oxidizing Al surface, inhibiting cathode corrosion at high voltage.[126] Employing a comparable strategy of fluorination on the central carbon chain, 2,2-difluoro-1,3-dimethoxypropane (FDMP) and 1,1,1-trifluoro-2,3-dimethoxypropane (TFDMP) also demonstrate exceptional high-voltage tolerance.[127,128] However, FDMB-based electrolytes may experience a progressively increasing overpotential during long-term cycling, which is likely attributable to the limited dissociation degree of Li^+ and anions resulting from the unique solvation structure of FDMB and Li^+ (Fig. 7b). Although such "weak dissociation" facilitates the formation of an anion-derived SEI, it significantly compromises ion conductivity, which is detrimental to practical battery applications.

Compared with fluorination on the central carbon chain, terminal group fluorination, based on the DEE molecule, can reduce the molecular solvation ability while preserving the overall chelate coordination structure with Li^+, thereby not sacrificing the ionic conductivity. Therefore, the terminal fluorinated-DEE family (FnDEE, n = 3–6) achieves an optimal balance between electrode stability and high ion conductivity, enabling stable overpotential during cycling and roughly >140 cycles in fast-cycling anode-free Cu||microparticle-$LiFePO_4$ (LFP) industrial pouch cells (Fig. 7c).[129] Similarly, the introduction of terminal $-CF_3$ groups into glyme ether molecules can also result in favorable performance enhancements.[130,131] However, due to the weakened lithium-ion solvation, these fluorinated linear ethers encounter issues such as sluggish redox kinetics and inadequate reversibility during high-rate cycling. Introducing asymmetry into the ether solvents can significantly alter the solvation free energy (ΔG_{solv}), leading to a reduced solvation effect and enhanced lithium ion mobility (Fig. 7d). Hence, the asymmetric fluorinate 1-ethoxy-2-methoxyethane (FxEME, x = 1–3) solvents demonstrate significantly faster charge transfer kinetics and a substantially higher exchange current density (j_0) compared with the symmetric FnDEE solvents. Theoretical calculations suggest that asymmetric solvents possess more pronounced directional dipole moments (μ), consequently diminishing the solvent shielding effect. This enables a more favorable orientation of asymmetric FxEME ethers under electric field, facilitating faster Li^+ desolvation and reducing the resistance to charge transfer (Fig. 7e). Consequently, the F3EME-based electrolyte enables Li||NCM811 full cells to achieve a long cycle life (>550 cycles) under electric vertical take-off and landing (eVTOL) protocols, facilitating the application of LMBs in electric aviation.[132] Adopting a similar asymmetric structural design strategy, fluorinated 1-methoxy-3-ethoxypropane (FnEMP) and fluorinated 1-(*n*,*i*)-propoxy-2-ethoxyethane (F3PEE) also exhibit favorable performances.[133,134]

Although the fluorinated linear ethers described above exhibit significant performance improvements in LMBs, the presence of non-polar trifluoro ($-CF_3$) and difluoro ($-CHF_2$) substituted groups inevitably leads to a compromise in the ionic conductivity of the electrolyte. In contrast, monofluoro group ($-CH_2F$) with strong local polarity can promote more solvent molecules to participate in the solvation coordination of Li^+, thereby significantly enhancing the ionic conductivity without deteriorating the oxidation stability (Fig. 7f). Through molecular simulation and machine learning screening, highly symmetric linear ethers with multiple monofluoro-substituted groups exhibit relatively optimal performance.[135] Therefore, a series of monofluorinated linear ether solvents-based electrolytes, including 1,2-bis(2-fluoroethoxy) ethane (FDEE),[136] bis(2-fluoroethoxy) methane (BFEM),[137,138] and bis(2-fluoroethyl) ether (BFE),[139] demonstrates enhanced ionic conductivity and improved fast-charging performance. Apart from fluorination, theoretical calculations suggest that chlorination can achieve stronger interactions between Li^+ and anions.[140] Hence, 1,2-bis(2-chloroethoxy)-ethyl ether (Cl-DEE) demonstrates favorable electrochemical performance, while possessing flame retardancy attributed to the readily generated $Cl^•$ that can effectively capture the highly active $H^•$ and inhibit the combustion progress (Fig. 7g).[141] It should be noted that the salt-dissolving capacity of solvent molecules inevitably diminishes with increasing fluorination. Consequently, many highly fluorinated or fully fluorinated hydrofluoroether molecules

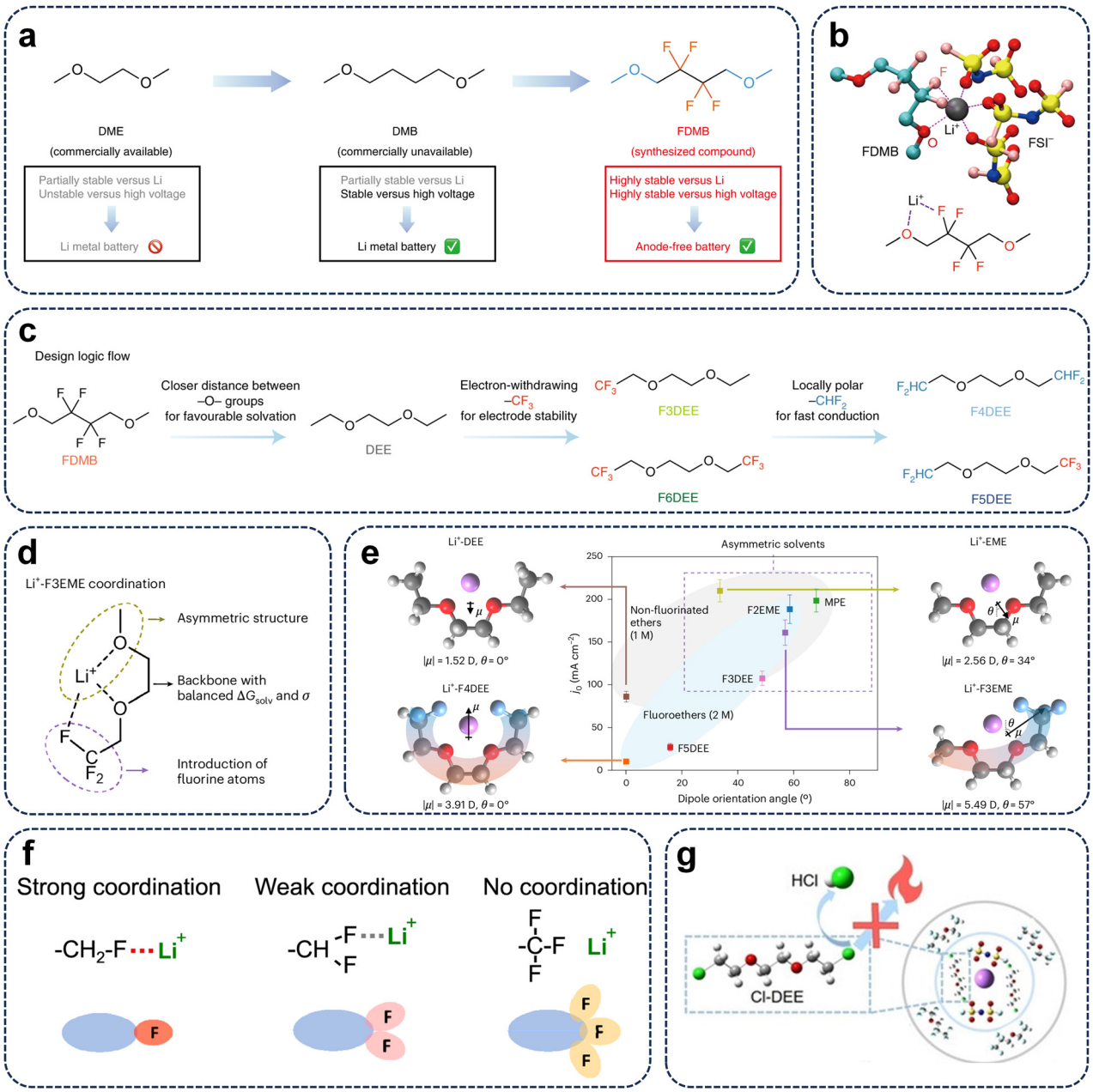

Fig. 7 (a) Design scheme of FDMB and (b) the solvation structure of 1 M LiFSI/FDMB. Reproduced with permission.[29] Copyright 2020, Springer Nature. (c) Logical flow for the design of the fluorinated-DEE family (FnDEE). Reproduced with permission.[129] Copyright 2022, Springer Nature. (d) Favorable characteristics of F3EME-based electrolyte towards high-rate Li-metal batteries. (e) Theoretical calculations of ion-induced dipole moment of Li^+-coordinated ether solvents, including DEE, EME, F4DEE, and F3EME, and positive correlation between dipole orientation angle and exchange current density within each class of solvent. Reproduced with permission.[132] Copyright 2025, Springer Nature. (f) Coordination chemistry of monofluoride, difluoro, and trifluoro groups. Reproduced with permission.[139] Copyright 2023, Springer Nature. (g) Schematic illustrations of the flame-retardant mechanism of Cl-DEE-based electrolyte. Reproduced with permission.[141] Copyright 2022, Wiley-VCH.

exhibit extremely low dielectric constants, making them unsuitable as primary solvents for dissolving lithium salts and preventing their participation in the Li^+ primary solvation shell. These fluorinated ether molecules are typically employed as diluents to improve the ionic conductivity of highly concentrated electrolytes and extend their electrochemical stability window.[142,143] Given that this review focuses on molecules that can function directly as solvents, such hydrofluoroether diluents will not be elaborated upon in this section. Nevertheless, through the design of asymmetric molecular structures, certain fluorinated linear ether diluents exhibit a weak coordination ability with Li^+, thereby enabling precise adjustment of core–shell-like solvation structures due to their amphiphilic properties.[144–146]

4. Other solvents containing heteroatoms

Apart from esters and ethers, the two predominant types of solvents, numerous other solvents containing heteroatoms in their molecular structure also exhibit potential for application in the electrolytes for LMBs due to the unique effects imparted by their distinct functional groups. In this section, we will review the research advancements of representative heteroatom-containing solvents, including nitriles, amides, sulfones, phosphates, and siloxanes.

4.1. Nitrogenous solvents

4.1.1. Nitrile solvents. Owing to the distinctive structure of the cyano group, nitrile solvents can effectively improve the high-voltage resistance of the electrolytes. The triple bond in the cyano group results in high bond energy, confining the electrons to the low-energy HOMO, which endows nitriles with exceptional oxidative stability and makes them compatible with most high-voltage cathode materials.[147] The cyano group can coordinate with transition metal ions, deactivating the catalytic activity of metal sites.[148] In addition, nitrile molecules exhibit superior solvation capabilities attributed to their relatively high dielectric constant. Concurrently, the potent coordination ability of the cyano group effectively facilitates the efficient transport of Li^+, thereby significantly enhancing the ionic conductivity of the electrolyte.[149] Therefore, nitrile solvents have extensive applications in fast-charging LIBs.[150,151] However, due to the strong unsaturation of the cyano group, which renders it prone to accepting electrons and undergoing reductive reactions, nitrile molecules exhibit poor compatibility with lithium metal and are commonly employed as a minor additive in LMBs.[152,153] By increasing the concentration of lithium salt and incorporating functional additives, the inherent limitations of nitrile solvents can be mitigated to a certain extent.[154–156] Unfortunately, this strategy fails to overcome the fundamental drawbacks of the nitrile solvents at the molecular level. In contrast to the traditional nitrile molecules using the cyano group as the main functional group, such as acetonitrile (AN) and succinonitrile (SN), introducing cyano groups as electron-withdrawing substituents into ether molecules in replacement of the fluorine atoms represents a promising approach to improve the reductive stability of nitrile solvents.[157] Compared with fluorine, the cyano group exhibits a milder electron-withdrawing effect, which will not significantly reduce the solvating power of ether solvents. Moreover, the cyano group and ether oxygen can form a chelating structure with Li^+, enhancing the dissociation of lithium salts, and the reduction of the cyano group can generate N-containing SEI on LMA, promoting rapid Li^+ migration and dense lithium deposition. Hence, ethylene glycol bis(propionitrile) ether (AN2-DME)-based electrolyte containing FEC demonstrates superior compatibility with LMA. Additionally, AN2-DME-based electrolyte can effectively remove the trace H_2O and HF in the electrolyte, restrain the PF_5-catalyzed decomposition of FEC, and form a uniform CEI that suppresses the dissolution of Ni^{4+} and HF attack (Fig. 8a).[158] Substituting the linear ether chain with a hexacyclic ether, 4-cyanotetrahydropyran (CNTHP) achieves a unique non-chelating ligand with Li^+, wherein the nitrogen atom acts as the primary coordination site, facilitating the formation of a robust SEI and enabling exceptional performance of LMBs (Fig. 8b).[159] In addition, simultaneously incorporating both the fluorine atom and the cyano group as substituents into the ether molecule can also achieve acceptable results.[160]

4.1.2. Amide solvents. Compared with other solvents, amide solvents exhibit a significant advantage in terms of their non-flammability. At elevated temperatures, amide solvents can generate $NCO^{\bullet}$ radicals, which can effectively terminate the chain propagation reactions and scavenge $H^{\bullet}$ and $HO^{\bullet}$ radicals, inhibiting the occurrence of combustion.[161] However, similar to carboxylate esters, amide solvents possess a carbonyl carbon with partial positive charge, which results in relatively poor reductive stability. Fortunately, compared with the widely used ester solvents, amide solvents are anticipated to form fewer low-ion-conductive inorganic compounds, such as Li_2O and Li_2CO_3, due to absence of the ester functional groups. Simultaneously, the presence of nitrogen renders amide molecules susceptible to reduction into Li–N compounds with high Li^+ conductivity, which mitigates the increase in interfacial resistance during cycling.[24] Therefore, amide solvents can be utilized in LMBs employing the LHCE strategy for their excellent film-forming ability and safety. As a representative, dimethylacetamide (DMAC) exhibits a high flash point (66 °C), ensuring the compatibility between cycling stability under practical conditions and nonflammability of electrolytes in LHCE.[161] Similarly, cyclic amide butyrolactam (BL) can promote the *in situ* formation of SEI with an abundance of LiF, Li_3N, and Li–N–C species, enabling stable cycling of LMBs at 60 °C.[162] By introducing the $-CF_3$ group, 2,2,2-trifluoro-*N*,*N*-dimethylacetamide (FDMA) exhibits lowered LUMO and HOMO levels, enhancing its oxidative stability and simultaneously enabling FDMA to participate in SEI formation at higher potentials. Attributed to the conjugation between the lone pair electron of the amino nitrogen and the π electron from the carbonyl group, the electron density on the nitrogen is reduced, making it more susceptible to accepting electrons. Therefore, FDMA will generate small-molecule compounds including Li_3N through a three-step decomposition mechanism without undergoing further reactions (Fig. 8c). Benefiting from the Li–N species with higher ionic conductivity, denser lithium deposits and top-down stripping are observed in FDMA-based electrolyte, which is in stark contrast to the porous deposition and homogeneous stripping alongside the formation of isolated regions of lithium metal and a larger amount of decomposition reactions in traditional carbonate electrolyte.[163] Furthermore, FDMA can be employed in highly fluorinated electrolytes as a shielding agent, demonstrating exceptional cycling stability and safety performance.[164,165] In particular, when a alkyl group on the nitrogen is replaced by a proton, the resulting amide molecule can form a deep eutectic

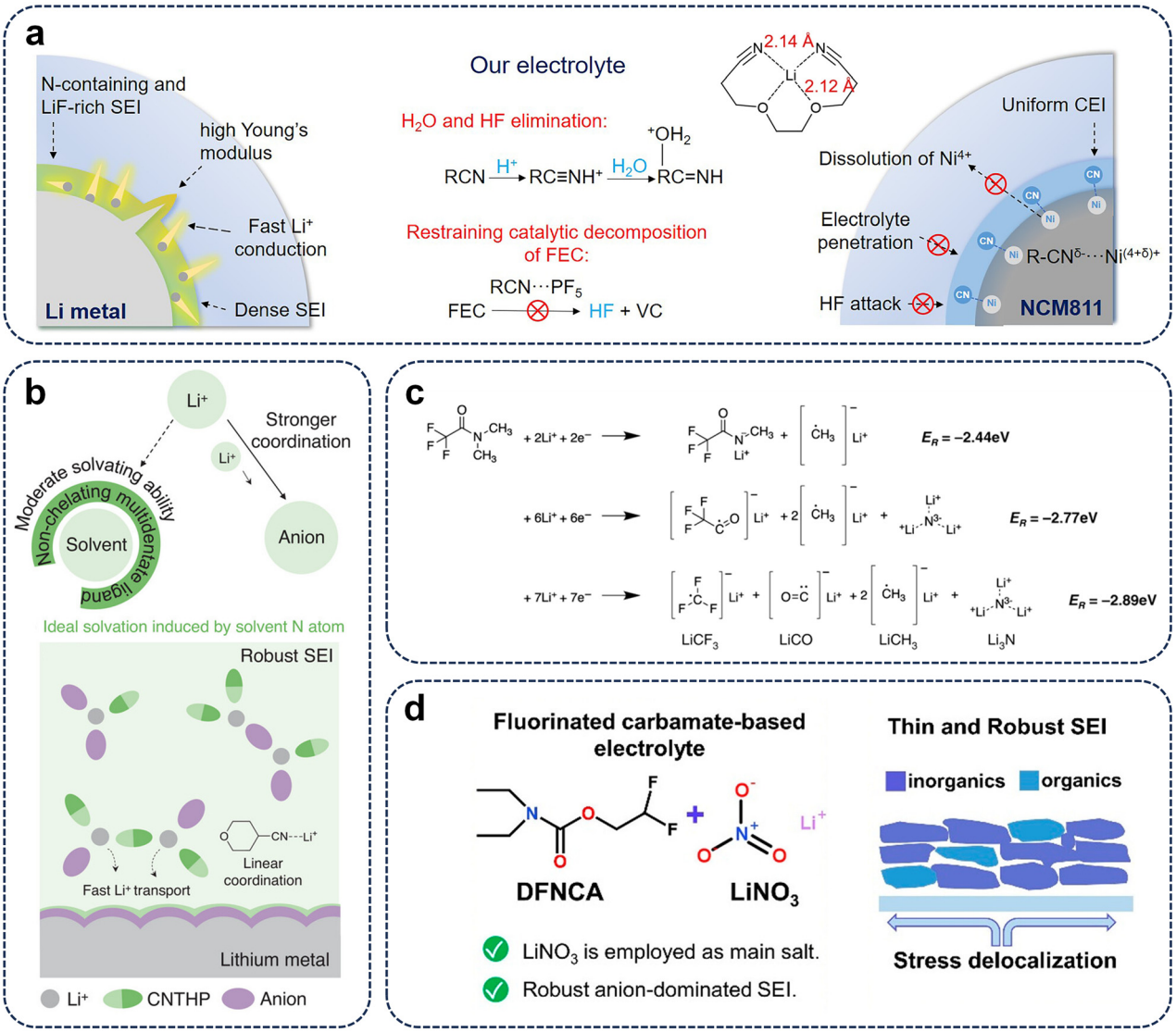

Fig. 8 (a) The chelating coordination structure of AN2-DME with Li^+, and schematic illustration highlighting the superiorities of AN2-DME-based electrolyte. Reproduced with permission.[158] Copyright 2024, National Academy of Sciences. (b) Schematics of Li^+ solvation behavior and SEI evolution in CNTHP-based electrolyte. Reproduced with permission.[159] Copyright 2025, Wiley-VCH. (c) Possible chemical reactions of FDMA on lithium metal surface. Reproduced with permission.[163] Copyright 2020, Springer Nature. (d) Schematic representation of the design concept of DFNCA. Reproduced with permission.[168] Copyright 2023, American Chemical Society.

electrolyte *via* hydrogen bonding with lithium salts, thereby further enhancing the safety. By incorporating additives or modifying lithium salts, potential adverse reactions between active hydrogen and lithium metal can be effectively mitigated. Consequently, these amide-based deep eutectic electrolytes demonstrate favorable performance.[166,167]

4.1.3. Carbamate solvents. Similar to the structure of carbonates, carbamate molecules simultaneously possess amide and ester functional groups, leading to poor reductive stability and inadequate SEI-forming capability, characterized by high resistance and lack of protective properties. Consequently, carbamate solvents typically necessitate the incorporation of film-forming additives like FEC, thus garnering limited attention in the electrolytes of LMBs. Fortunately, benefiting from the relatively high donor number of ~17.5, carbamates can facilitate the solvation of some LMA-friendly lithium salts, such as $LiNO_3$, whose solubility could be increased to 0.5 M in 2,2-difluoroethyl *N*,*N*-diethyl carbamate (DFNCA). Hence, adopting $LiNO_3$ as the main salt, along with lithium difluoro(oxalato)borate (LiDFOB) and FEC as additives, DFNCA-based electrolyte demonstrates favorable electrochemical performance (Fig. 8d).[168] Similarly, cyclic carbamate 3-methyl-2-oxazolidinone (MOX) also demonstrates enhanced $LiNO_3$-dissolving ability, enabling Li||LFP and Li||NCM622 cells to stably cycle for over 1000 cycles.[169,170]

4.2. Sulfurous solvents

4.2.1. Sulfone solvents. Attributed to their extremely low HOMO levels, sulfone solvents possess exceptionally high oxi-

dative stability, making them a common choice to be adopted in high-voltage electrolytes.[171] As a representative, sulfolane (SL) exhibits a high oxidative decomposition voltage exceeding 5 V (*vs.* Li^+/Li), along with a high flash point (166 °C), enhancing the safety profile of the batteries.[172,173] However, the strong electron-withdrawing nature of the highly polar sulfonyl group endows sulfone solvents with high viscosity and insufficient wettability toward the electrodes and separators.[174] Moreover, sulfone solvents exhibit poor compatibility with LMA, leading to the formation of a highly resistive SEI along with the shuttling RSO_2^- and RSO_3^- species, which consequently causes a significant increase in charge transfer resistance.[32] Hence, the application of sulfone solvents in LMBs is restricted. Some research studies have shown that implementing the LHCE strategy can improve the compatibility of SL-based electrolytes with LMA, but the Li plating/stripping CE remains limited to below 99%.[175,176] Nevertheless, the strong electron-withdrawing nature of sulfonyl group also leads to sufficient dissociation of lithium salts, enabling SL to readily dissolve LMA-compatible lithium salts, such as $LiNO_3$ and LiDFOB, thus enhancing the cycling stability of LMBs using conventional concentration lithium salts.[177,178] In particular, some sulfone molecules featuring unique unsaturated structures, such as butadiene sulfone (BDS) and prop-1-ene-1,3-sultone (PES), can be utilized to construct deep eutectic electrolytes, achieving satisfactory outcomes.[179,180] In general, the application of sulfone molecules in the electrolytes of LMBs is limited.

4.2.2. Sulfamide solvents. LiFSI and lithium bis(trifluoromethanesulfonyl)-imide (LiTFSI) are the two predominant lithium salts utilized in the electrolytes of LMBs, attributed to their unique fluoro sulfamide group, which possesses strong electron-withdrawing effect, enhancing the dispersion of negative charges and reducing ion pairing to improve the solubility of the salts. In addition, they exhibit excellent thermostability along with high ionic conductivity, and have a tendency to decompose on anodes to form a robust SEI rich in inorganic lithium salts.[181] Inspired by this, a salt-structure-mimicking strategy has been proposed and a series of sulfamide solvents featuring a fluoro sulfamide structure has been developed for LMBs. *N*,*N*-dimethylsulfamoyl fluoride (DMSF) exhibits a structural similarity to LiFSI, the F atom of which is more conducive to the formation of LiF on the LMA surface compared with FEC, enabling uniform and compact lithium deposits (Fig. 9a).[182] Likewise, *N*,*N*-dimethyltrifluoromethane-sulfonamide (DMTMSA), which possesses a molecular structure similar to LiTFSI, can not only effectively suppress side reactions, transition-metal dissolution, stress-corrosion cracking, and impedance growth on the cathode, but can also facilitate highly reversible lithium stripping and plating, resulting in a compact morphology and minimal pulverization (Fig. 9b). Hence, DMTMSA-based electrolyte can achieve a high cut-off voltage of 4.7 V in Li||NCM811 cells.[183] Additionally, it can also inhibit the surface degradation, detrimental gas evolution, and Co dissolution on $LiCoO_2$ (LCO) cathode, enabling over 200 cycles of Li||LCO cells.[184] By extending the fluorine chain, the solvation capability of the sulfamide solvents is reduced. The bipolar nonafluoro-*N*,*N*-dimethylbutane sulfonamide (NFS) features an ion-dissociative polar head and a perfluorinated nonpolar tail. The unique structure enables the formation of capsule-like solvation sheaths through weak coordination, effectively encapsulating polar molecules within the primary solvation shell and thereby significantly reducing the detrimental decomposition of the solvents (Fig. 9c). Therefore, NFS-based electrolyte can achieve a high energy density of 440 Wh kg^{-1} in pouch cells.[185] Other than extending the fluoro chain, replacing the dimethylamino group with a cyclic amino group can also modulate the steric and electronic properties, thereby enabling enhanced contact ion pairs for the formation of an anion-derived SEI (Fig. 9d). Consequently, *N*-azetidine-trifluoromethanesulfonamide (TFSAT), *N*-pyrrolidine-trifluoromethanesulfonamide (TFSPY), *N*-piperidine-trifluoromethanesulfonamide (TFSPP), and *N*-morpholine-trifluoromethanesulfonamide (TFSMP) all demonstrate excellent compatibility with both LMA and high-voltage cathodes.[186–188]

4.3. Phosphate solvents

Phosphate molecules are widely employed as highly effective flame-retardant additives in LIBs/LMBs.[189,190] They can inhibit combustion *via* radical elimination reactions, thereby effectively suppressing the chain reactions that sustain combustion.[191] Taking the commonly used trimethyl phosphate (TMP) and triethyl phosphate (TEP) as examples, liquid TMP/TEP evaporates into the gaseous phase in the flame environment and undergoes thermal decomposition to generate phosphorus-containing free radicals like $PO^•$, which subsequently combines with $H^•$ and $HO^•$ species to effectively suppress the combustion process. However, due to the incompatibility of phosphate solvents with LMA, it is challenging to utilize them as primary solvents in LMBs unless the solvation structure is precisely optimized or functional additives are introduced.[192–195] By introducing specific functional groups, it is expected that molecular-level optimization of phosphate solvents will be achieved. Inspired by the highly stable DME, an ether-functionalized phosphate molecule, diethyl (2-methoxy ethoxy) methyl phosphonate (DMEP), has been proposed (Fig. 9e). The incorporation of the DME segment enhances the dielectric constant of DMEP, thereby increasing the stability of the AGG-dominated solvation structure and avoiding the salt precipitation in TEP-based LHCE. Therefore, DMEP-based electrolyte demonstrates an enhanced SEI-forming ability and alleviated structural degradation of the NCM811 cathode at 4.7 V, while simultaneously maintaining excellent safety characteristics.[196] As mentioned above, the cyano group exhibits strong complexation with transition metals, effectively inhibiting their dissolution and thereby ensuring the structural stability of the cathode. Hence, by incorporating a cyano group into the phosphate molecule, diethyl (2-cyanethyl) phosphonate (DCEP) can form a stable seven-membered chelating structure with Li^+, which facilitates the formation of an inorganic-rich electrode–electrolyte interphase with high robustness, thus enabling the outstanding cycling stability of Li||NCM811 cells (>300 cycles) (Fig. 9f).[197] The fluorination strategy demon-

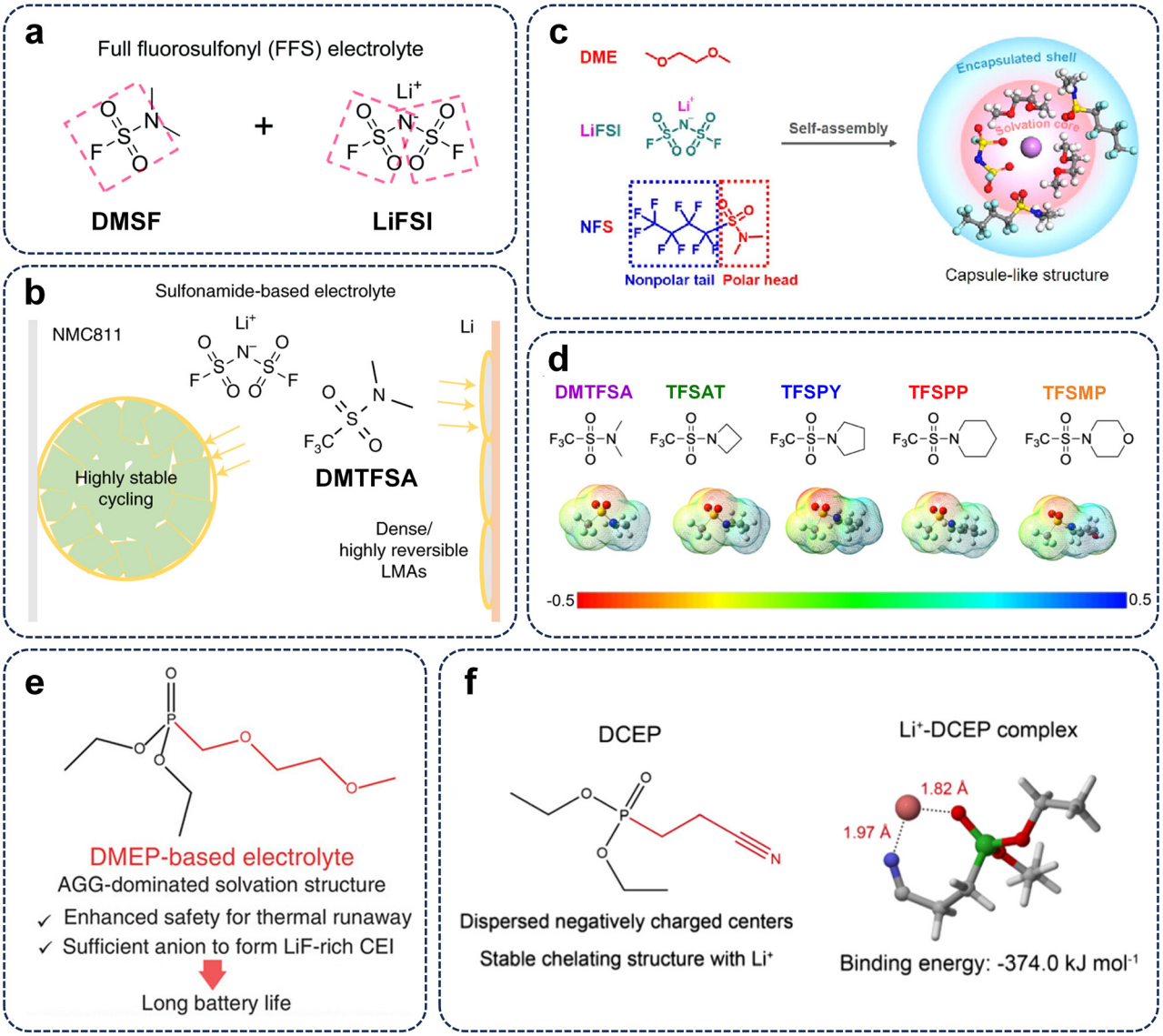

Fig. 9 (a) The molecular structures of DMSF and LiFSI. Reproduced with permission.[182] Copyright 2019, The Royal Society of Chemistry. (b) The DMTFSA-based electrolyte that promotes dense lithium deposits and inhibits the intergranular cracking of NCM811 cathode. Reproduced with permission.[183] Copyright 2021, Springer Nature. (c) Molecular design principle of the bipolar NFS molecule and the corresponding capsule-like solvation structure. Reproduced with permission.[185] Copyright 2023, American Chemical Society. (d) Molecular structure and ESP mapping of DMTFSA, TFSAT, TFSPY, TFSPP, and TFSMP. Reproduced with permission.[188] Copyright 2025, American Chemical Society. (e) Molecular structure and superiorities of DMEP. Reproduced with permission.[196] Copyright 2024, Wiley-VCH. (f) Molecular structure of DCEP and the seven-membered chelating structure of Li^+-DCEP. Reproduced with permission.[197] Copyright 2024, American Chemical Society.

strates comparable efficacy for phosphate molecules, which not only optimizes the SEI but also markedly enhances high-voltage stability. Consequently, 2-(2,2,2-trifluoroethoxy)-1,3,2-dioxaphospholane 2-oxide (TFEP)- and (2-trifluoroethoxy ethyl) bis(trifluoroethoxy) phosphate (FEBFP)-based electrolytes can enable stable cycling of Li||$LiMn_{1.5}O_4$ (LMO) or Li||LNMO cells with a high cutoff voltage (>4.9 V).[198,199]

4.4. Siloxane solvents

Siloxane molecules are distinguished by Si–O bonds, where the silicon atom possesses 3d empty orbitals that can accept the lone pair electron from the adjacent oxygen atom, thereby forming a d-p conjugation analogous to p–π conjugation in ester molecules. The energy level of the molecular orbital formed *via* Si–O conjugation is substantially lower than that of the initial oxygen atomic orbital. This results in a greater confinement of non-bonding electrons and a significantly reduced HOMO energy level in siloxanes compared with ethers, significantly enhancing their oxidative stability (Fig. 10a).[200] In addition, owing to their structural similarity to ethers, siloxanes exhibit excellent compatibility with LMA. The conjugation effect additionally results in the Si–O bond possessing a

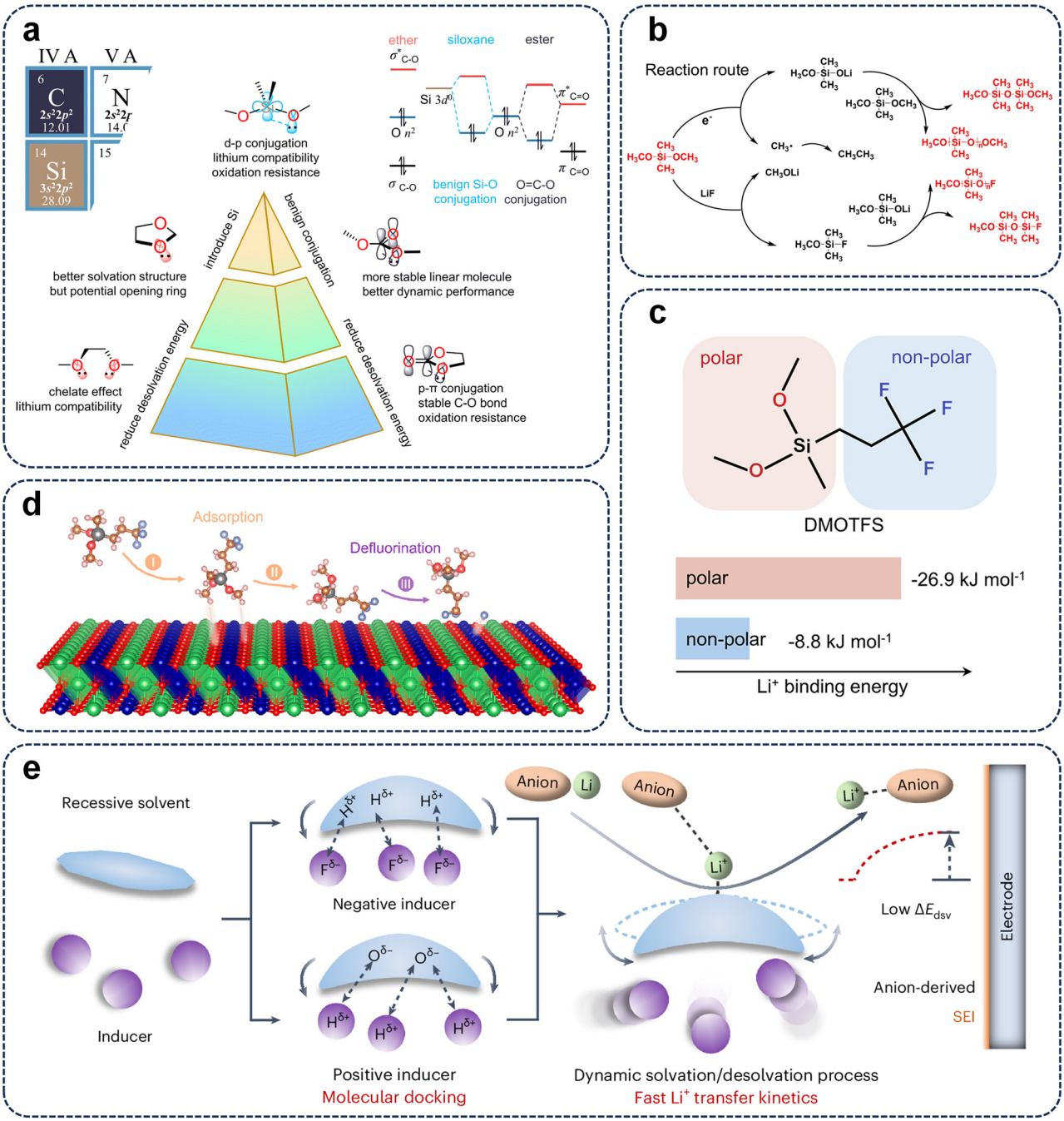

Fig. 10 (a) Molecular design principles of siloxane solvents. Reproduced with permission.[200] Copyright 2022, The Royal Society of Chemistry. (b) Diagram of the generation mechanism of silicone-containing organic SEI. Reproduced with permission.[201] Copyright 2025, Elsevier. (c) Chemical structure of DMOTFS and the binding energies of different segments with Li^+. Reproduced with permission.[204] Copyright 2023, American Chemical Society. (d) Mechanism analysis of the adsorption-defluorination process of DMOTFS molecules on the LCO cathode. Reproduced with permission.[206] Copyright 2023, American Chemical Society. (e) Li^+ solvation mechanism in molecular-docking electrolytes. Reproduced with permission.[208] Copyright 2024, Springer Nature.

higher flexible force constant compared with the C–O bond, which suggests that siloxanes have superior chemical stability. Therefore, dimethyl dimethoxy silane (DMMS)-based electrolytes demonstrate outstanding performance, enabling 1.4 Ah-level Li||NCM811 pouch cell to cycle stably for 140 cycles with a capacity retention of 96%. Additionally, the DMMS-based electrolyte facilitates the formation of an organic SEI enriched with Si–O species, which has rapid ion transport kinetics and superior mechanical stability (Fig. 10b). Compared with a traditional organic SEI containing $ROCO_2Li$ and ROLi, such a Si-rich SEI exhibits less decomposition and reconstruction during long-term operation, thereby significantly enhancing

the cycling stability under low-temperature conditions and enabling the Li||NCM811 cell to retain its discharge capacity even at an extremely low temperature of −114.05 °C.[201]

Fluorination further enhances the oxidative stability of siloxane molecules while modifying the solvation structure. 3,3,3-trifluoropropyl trimethoxy silane (TFTMS)-based electrolyte possesses higher ionic conductivity compared with DMMS-based electrolyte, accelerating the reaction kinetics.[202] Meanwhile, the weakly solvating ability of TFTMS facilitates the stabilization of solvation structures enriched in anions, effectively suppressing dissolution of lithium polysulfides and thereby endowing Li/FeS_2 cells with a long lifespan (>4000 h).[203] As a semisolvated solvent, 3,3,3-trifluoropropyl methyl dimethoxy silane (DMOTFS) integrates both solvated and non-solvated fragments within a single molecule, minimizing the saturation concentration of lithium salts and constructing a solvation structure akin to that of LHCEs with a moderate lithium salt concentration (Fig. 10c).[204] Meanwhile, DMOTFS can enhance the decomposition extent of LiFSI, enriching SEI with LiF rather than S–F species, and thus facilitating the stable cycling of LMBs.[205] In addition, in Li||LCO cells, DMOTFS tends to adsorb onto the surface of the LCO cathode, triggering the sacrificial release of F atoms and consequently forming a passivation layer that suppresses the catalytic activity of the electrolyte (Fig. 10d). Therefore, the DMOTFS-based electrolyte can also enable stable long-term cycling of Li||LCO cells for 250 cycles with a cutoff voltage of 4.6 V.[206]

Through hypermethylation, some other siloxane molecules containing two silicon atoms demonstrate reduced solvating ability and outstanding performances. Tetramethyl-1,3-dimethoxydisiloxane (TMMS) features a fully methylated structure, which can effectively increase the dehydrogenation energy barrier, further mitigating the oxidative decomposition of the electrolyte.[207] As recessive solvents incapable of dissolving lithium salts, 1,2-bis(trimethylsilyloxy)ethane (BTE) and 1,3-bis(trimethylsilyloxy)propane (BTP) can construct molecular-docking electrolytes with the assistance of inducers, such as fluorinated benzene and halide alkane compound, driven by an atypical hydrogen bond effect. Such a hydrogen bond effect can lead to the conformational change of the recessive solvents, concurrently lowering their electrostatic potential and promoting Li^+ solvation. Therefore, the molecular-docking electrolytes exhibit a dynamic Li^+-solvent solvation/desolvation process driven by the dynamic inducer-recessive solvent docking/undocking process, which significantly enhances the desolvation kinetics (Fig. 10e). Consequently, the BTP-based electrolyte endows Li||NCM811 cells with ultra-long lifespan (700 cycles with a capacity retention of 90%).[208]

5. Summary and outlook

The design of solvent molecular structures plays a crucial role in constructing advanced electrolyte systems for LMBs. The integration of functional groups with distinct functionalities at the molecular level can compensate for the intrinsic deficiencies of solvent molecules, markedly enhancing their adaptability, which remains unattainable through the simple physical blending of different solvents. This review systematically summarizes recent advances in the design of novel electrolyte solvents for LMBs, critically evaluates the strengths and limitations of various solvent molecules including esters, ethers, nitrogenous solvents, sulfones/sulfamides, phosphates, and siloxanes, and distills fundamental design principles. The distinct characteristics of various solvent types are summarized in Fig. 11. The primary molecular modification strategies currently employed encompass fluorination, adjustment of the main-chain length, modulation of steric hindrance, incorporation of functional branches, and synergistic integration of multiple functional groups. It can be detected that novel electrolytes can be intrinsically designed with multi-functionality and high performance through rational molecular structure optimization. This can also effectively circumvent cost-related issues arising from complex electrolyte formulation and the ambiguity associated with synergistic mechanisms of various components.

Certainly, the design of new solvent molecules necessitates comprehensive consideration of different properties to satisfy compatibility with the LMA and the prospects for practical applications, including both oxidative and reductive stability, sufficient salt solubility, a wide liquid temperature range, cost-effective and straightforward synthesis methods, as well as adequate safety. Unfortunately, although a variety of novel solvent molecules have been proposed, most still suffer from unavoidable intrinsic limitations, such as the insufficient reductive stability of esters and the inadequate oxidative stability of ethers. Therefore, continued efforts are still required to deepen the comprehensive understanding of the molecular design principles in order to address these challenges in future research, and the following design concepts need to be carefully considered.

(1) As a representative molecular modification strategy, fluorination can modulate the electron cloud distribution of molecules through the electron-withdrawing effect of fluorine atoms. This leads to enhanced oxidative stability and the formation of a fluorine-rich interfacial layer on the anode side, thereby substantially improving the electrochemical performance of the solvent. Moreover, fluorine atoms can efficiently bind to hydrogen radicals, thereby interrupting the combustion chain reaction and reducing the likelihood of thermal runaway in batteries. However, the associated high cost and environmental concerns have limited practical commercial application of fluorination. The research focus should be placed on low-cost and environmentally friendly non-fluorinated molecules, with the attempt to utilize the steric effect or the synergistic interactions of multiple functional groups, thus achieving effects comparable to fluorination.

(2) Most solvent molecules are unable to simultaneously satisfy the dual requirements of reductive stability and oxidative stability. For instance, ester solvents typically require

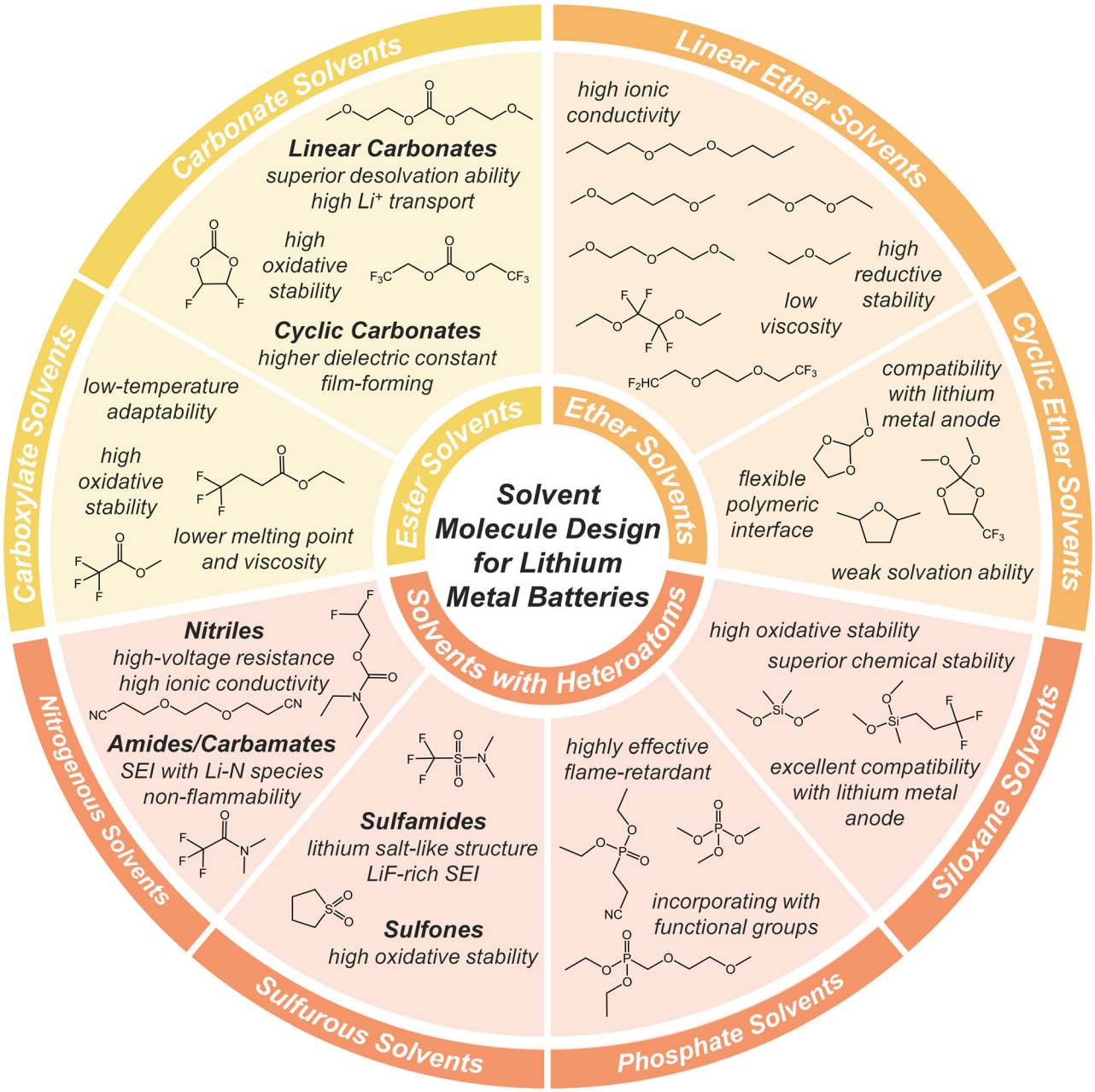

Fig. 11 The distinct characteristics of various types of solvent molecules.

film-forming additives such as FEC to facilitate the formation of a stable SEI layer that suppresses continuous side reactions at the anodes, and ether solvents frequently necessitate the implementation of the LHCE strategy to improve the overall high-voltage tolerance of the electrolyte. Owing to the unique conjugation effect of the Si–O bond, siloxane molecules are among the few solvents that exhibit excellent oxidation and reduction stabilities simultaneously, and are therefore considered as a promising direction for the development of next-generation solvents.

(3) Through molecular structural modification, the cycling stability and wide-temperature performance of the electrolytes have been significantly improved, while solvents that can simultaneously achieve high safety remain scarce. During the early stage of battery operation, abusive conditions may induce decomposition of organic solvents, leading to a rapid temperature increase and potentially triggering thermal runaway. Upon battery rupture, internally released combustible gases can readily react with ambient oxygen, resulting in immediate ignition or even explosion. Therefore, solvent screening should prioritize critical safety parameters, including boiling/flash point, thermal stability, and inherent flame-retardant properties, to ensure overall battery safety. Extending the molecular chains can enhance the intermolecular contact area,

thereby strengthening the intermolecular forces, which in turn effectively increases the boiling/flash points. Under high-temperature conditions phosphates and fluorinated solvents are capable of generating free radicals, such as $PO^{\bullet}$ and $F^{\bullet}$, which can effectively react with $H^{\bullet}$ and $OH^{\bullet}$ produced during the decomposition of organic solvents, thereby interrupting the chain reaction and preventing combustion. Furthermore, siloxanes exhibit excellent inherent thermal stability and can be activated by metallic lithium under high-temperature conditions to undergo condensation reactions, leading to the formation of a thermally stable polysiloxane network.[209] Consequently, these solvents demonstrate favorable safety characteristics, and when combined with optimized electrochemical performance, they hold great potential for enabling practical and inherently safe LMBs.

(4) Given the vast diversity of solvent molecules, conducting individual testing and screening for each one is exceedingly labor-intensive and impractical. By leveraging machine learning, various molecules can be efficiently processed through batch theoretical calculations and molecular dynamics simulations, allowing for the systematic acquisition of physical and chemical properties at the theoretical level, which effectively supports the molecular design and screening.[210–213] Deep learning can transform molecular structures into mathematical features (vectors) that are interpretable by machine learning models through graph neural networks or the extraction of physicochemical descriptors, thereby enabling high-throughput molecular screening. By analyzing the multidimensional parameters of each molecule in a virtual database, key indicators of interest to researchers—such as potential solvation structures, SEI compositions, and electrochemical properties—can be predicted. This approach allows for a significant and efficient reduction in the pool of solvent candidates, thereby streamlining the screening and formulation of solvents and electrolytes. Nevertheless, machine learning remains heavily reliant on databases, making the construction of high-quality and standardized datasets continue to be the primary challenge. Efforts from data-sharing communities and automated experimental platforms are currently addressing this issue. Furthermore, most current machine learning models focus on predicting final performance based on initial states, but the modeling of complex dynamic interfacial evolution during battery cycling remains in its early stages.

(5) Despite achieving excellent electrochemical performance, liquid electrolytes still have the inherent defect of flammability. Compared with liquid electrolytes, solid electrolytes are non-flammable and exhibit sufficient mechanical strength to inhibit the penetration of lithium dendrites, thereby significantly enhancing battery safety. Furthermore, solid-state batteries can be designed with a compact bipolar stacking configuration, enabling the integration of more active materials within a limited volume, which leads to improved energy density and a simplified battery pack structure. Consequently, solid electrolytes hold promising potential as an alternative to liquid electrolytes in future lithium metal batteries. However, apart from a few sulfide-based materials, most solid electrolytes suffer from low room-temperature ionic conductivity and various interfacial challenges, which hinder their electrochemical performance. Additionally, their fabrication often involves complex processes, such as high-temperature sintering, resulting in higher production costs and incompatibility with existing battery manufacturing lines. Therefore, significant efforts are still required to overcome these barriers and realize the practical application and industrialization of solid electrolytes.

Author contributions

X. Zhu conducted the literature search, conceived the overall structure of the review, and wrote the manuscript. X. Dong proposed the topic of the review and revised the manuscript. All the authors participated in the discussion and revision of the manuscript.

Conflicts of interest

There are no conflicts to declare.

Data availability

No primary research results, software or code have been included and no new data were generated or analysed as part of this review.

Acknowledgements

This work was supported by the National Key Research and Development Program of China (No. 2022YFB3803400), the National Natural Science Foundation of China (No. 22379028 and 22109028), and the Natural Science Foundation of Shanghai (No. 22ZR1404400).

References

1 C. P. Grey and D. S. Hall, *Nat. Commun.*, 2020, **11**, 6279.
2 F. Duffner, N. Kronemeyer, J. Tübke, J. Leker, M. Winter and R. Schmuch, *Nat. Energy*, 2021, **6**, 123–134.
3 L. Li, D. Zhang, J. Deng, Y. Gou, J. Fang, H. Cui, Y. Zhao and M. Cao, *Carbon*, 2021, **183**, 721–734.
4 N. Kim, Y. Kim, J. Sung and J. Cho, *Nat. Energy*, 2023, **8**, 921–933.
5 Y. Liu, H. Shi and Z.-S. Wu, *Energy Environ. Sci.*, 2023, **16**, 4834–4871.
6 M. Ue and K. Uosaki, *Curr. Opin. Electrochem.*, 2019, **17**, 106–113.
7 K. Park, J. Song and K. T. Lee, *Batteries Supercaps*, 2023, **6**, e202300344.

8 M. He, L. G. Hector Jr, F. Dai, F. Xu, S. Kolluri, N. Hardin and M. Cai, *Nat. Energy*, 2024, **9**, 1199–1205.
9 Y. Jie, S. Wang, S. Weng, Y. Liu, M. Yang, C. Tang, X. Li, Z. Zhang, Y. Zhang, Y. Chen, F. Huang, Y. Xu, W. Li, Y. Guo, Z. He, X. Ren, Y. Lu, K. Yang, S. Cao, H. Lin, R. Cao, P. Yan, T. Cheng, X. Wang, S. Jiao and D. Xu, *Nat. Energy*, 2024, **9**, 987–998.
10 H. Raza, S. Bai, J. Cheng, S. Majumder, H. Zhu, Q. Liu, G. Zheng, X. Li and G. Chen, *Electrochem. Energy Rev.*, 2023, **6**, 29.
11 K. Chen, D.-Y. Yang, G. Huang and X.-B. Zhang, *Acc. Chem. Res.*, 2021, **54**, 632–641.
12 X. Guan, A. Wang, S. Liu, G. Li, F. Liang, Y.-W. Yang, X. Liu and J. Luo, *Small*, 2018, **14**, 1801423.
13 H. Wang, J. Liu, G. Jiang, J. Huang, D. Wu, G. Yang and J. Ma, *Adv. Energy Mater.*, 2024, **14**, 2400067.
14 W. Dachraoui, R.-S. Kühnel, C. Battaglia and R. Erni, *Nano Energy*, 2024, **130**, 110086.
15 Y. Liu, B. Yuan, C. Sun, Y. Lu, X. Lin, M. Chen, Y. Xie, S. Zhang and C. Lai, *Adv. Funct. Mater.*, 2022, **32**, 2202771.
16 Q. Wang, B. Liu, Y. Shen, J. Wu, Z. Zhao, C. Zhong and W. Hu, *Adv. Sci.*, 2021, **8**, 2101111.
17 Q.-K. Zhang, X.-Q. Zhang, H. Yuan and J.-Q. Huang, *Small Sci.*, 2021, **1**, 2100058.
18 H. Cheng, Q. Sun, L. Li, Y. Zou, Y. Wang, T. Cai, F. Zhao, G. Liu, Z. Ma, W. Wahyudi, Q. Li and J. Ming, *ACS Energy Lett.*, 2022, **7**, 490–513.
19 C. Tian, K. Qin and L. Suo, *Mater. Futures*, 2023, **2**, 012101.
20 M. Wang, M. Zheng, J. Lu and Y. You, *Joule*, 2024, **8**, 2467–2482.
21 Z. Wang and B. Zhang, *Energy Mater. Devices*, 2023, **1**, 9370003.
22 Y. Yang, Y. Yin, D. M. Davies, M. Zhang, M. Mayer, Y. Zhang, E. S. Sablina, S. Wang, J. Z. Lee, O. Borodin, C. S. Rustomji and Y. S. Meng, *Energy Environ. Sci.*, 2020, **13**, 2209–2219.
23 Z. Zhao, G. Melinte, Y. Lei, D. Guo, M. N. Hedhili, Z. Shi, H. Qasem and H. N. Alshareef, *ACS Energy Lett.*, 2025, **10**, 1129–1138.
24 Z. Li, Y. Chen, X. Yun, P. Gao, C. Zheng and P. Xiao, *Adv. Funct. Mater.*, 2023, **33**, 2300502.
25 D. Ruan, Z. Cui, J. Fan, D. Wang, Y. Wu and X. Ren, *Chem. Sci.*, 2024, **15**, 4238–4274.
26 J. Wang, J. Luo, H. Wu, X. Yu, X. Wu, Z. Li, H. Luo, H. Zhang, Y. Hong, Y. Zou, S. Cao, Y. Qiao and S.-G. Sun, *Angew. Chem., Int. Ed.*, 2024, **63**, e202400254.
27 M. Yeddala, L. Rynearson and B. L. Luchi, *ACS Energy Lett.*, 2023, **8**, 4782–4793.
28 Z. Piao, R. Gao, Y. Liu, G. Zhou and H.-M. Cheng, *Adv. Mater.*, 2023, **35**, 2206009.
29 Z. Yu, H. Wang, X. Kong, W. Huang, Y. Tsao, D. G. Mackanic, K. Wang, X. Wang, W. Huang, S. Choudhury, Y. Zheng, C. V. Amanchukwu, S. T. Hung, Y. Ma, E. G. Lomeli, J. Qin, Y. Cui and Z. Bao, *Nat. Energy*, 2020, **5**, 526–533.
30 Y. Liu, D. Lin, Y. Li, G. Chen, A. Pei, O. Nix, Y. Li and Y. Cui, *Nat. Commun.*, 2018, **9**, 3656.
31 Y. Xia, P. Zhou, X. Kong, J. Tian, W. Zhang, S. Yan, W.-H. Hou, H.-Y. Zhou, H. Dong, X. Chen, P. Wang, Z. Xu, L. Wan, B. Wang and K. Liu, *Nat. Energy*, 2023, **8**, 934–945.
32 Y. Wang, Z. Li, Y. Hou, Z. Hao, Q. Zhang, Y. Ni, Y. Lu, Z. Yan, K. Zhang, Q. Zhao, F. Li and J. Chen, *Chem. Soc. Rev.*, 2023, **52**, 2713–2763.
33 J. Wang, P. Kumar, Z. Ma, H. Liang, F. Zhao, H. Xie, Y. Wang, T. Cai, Z. Cao, L. Cavallo, Q. Li and J. Ming, *ACS Energy Lett.*, 2024, **9**, 4386–4398.
34 X. Zhang, P. Xu, J. Duan, X. Lin, J. Sun, W. Shi, H. Xu, W. Dou, Q. Zheng, R. Yuan, J. Wang, Y. Zhang, S. Yu, Z. Chen, M. Zheng, J.-F. Gohy, Q. Dong and A. Vlad, *Nat. Commun.*, 2024, **15**, 536.
35 J. Chen, D. Zhang, L. Zhu, M. Liu, T. Zheng, J. Xu, J. Li, F. Wang, Y. Wang, X. Dong and Y. Xia, *Nat. Commun.*, 2024, **15**, 3217.
36 S. Cao, X. He, L. Nie, J. Hu, M. Chen, Y. Han, K. Wang, K. Jiang and M. Zhou, *Adv. Sci.*, 2022, **9**, 2201147.
37 H. Wang, S. C. Kim, T. Rojas, Y. Zhu, Y. Li, L. Ma, K. Xu, A. T. Ngo and Y. Cui, *J. Am. Chem. Soc.*, 2021, **143**, 2264–2271.
38 Y. H. T. Tran, K. An, D. T. T. Vu and S.-W. Song, *ACS Energy Lett.*, 2025, **10**, 356–370.
39 E. Markevich, G. Salitra, F. Chesneau, M. Schmidt and D. Aurbach, *ACS Energy Lett.*, 2017, **2**, 1321–1326.
40 H. Li and Y. Li, *RSC Adv.*, 2024, **14**, 37074–37081.
41 P. Biswal, J. Rodrigues, A. Kludze, Y. Deng, Q. Zhao, J. Yin and L. A. Archer, *Cell Rep. Phys. Sci.*, 2022, **3**, 100948.
42 Z. Wang, Z. Sun, Y. Shi, F. Qi, X. Gao, H. Yang, H.-M. Cheng and F. Li, *Adv. Energy Mater.*, 2021, **11**, 2100935.
43 C.-C. Su, M. He, R. Amine, Z. Chen, R. Sahore, N. D. Rago and K. Amine, *Energy Storage Mater.*, 2019, **17**, 284–292.
44 P. Xiao, Y. Zhao, Z. Piao, B. Li, G. Zhou and H.-M. Cheng, *Energy Environ. Sci.*, 2022, **15**, 2435–2444.
45 L. Deng, L. Dong, Z. Wang, Y. Liu, J. Zhan, S. Wang, K.-P. Song, D. Qi, Y. Sang, H. Liu and H. Chen, *Adv. Energy Mater.*, 2024, **14**, 2303652.
46 S. Chen, Y. Xiang, G. Zheng, Y. Liao, F. Ren, Y. Zheng, H. He, B. Zheng, X. Liu, N. Xu, M. Luo, J. Zheng and Y. Yang, *ACS Appl. Mater. Interfaces*, 2020, **12**, 27794–27802.
47 W. Zhang, T. Yang, X. Liao, Y. Song and Y. Zhao, *Energy Storage Mater.*, 2023, **57**, 249–259.
48 W. Yang, Z. Zhang, X. Sun, Y. Liu, C. Sheng, A. Chen, P. He and H. Zhou, *Angew. Chem., Int. Ed.*, 2024, **63**, e202410893.
49 Z. Wang, Z. Li, J. Fu, S. Zheng, R. Yu, X. Zhou, G. He and X. Guo, *Green Energy Environ.*, 2024, **9**, 1601–1609.
50 X. Fan, X. Ji, L. Chen, J. Chen, T. Deng, F. Han, J. Yue, N. Piao, R. Wang, X. Zhou, X. Xiao, L. Chen and C. Wang, *Nat. Energy*, 2019, **4**, 882–890.
51 E. R. Logan, E. M. Tonita, K. L. Gering, J. Li, X. Ma, L. Y. Beaulieu and J. R. Dahn, *J. Electrochem. Soc.*, 2018, **165**, A21.

52 Y. Mo, G. Liu, Y. Yin, M. Tao, J. Chen, Y. Peng, Y. Wang, Y. Yang, C. Wang, X. Dong and Y. Xia, *Adv. Energy Mater.*, 2023, **13**, 2301285.
53 M. C. Smart, B. V. Ratnakumar and S. Surampudi, *J. Electrochem. Soc.*, 2002, **149**, A361.
54 Y. Feng, L. Zhou, H. Ma, Z. Wu, Q. Zhao, H. Li, K. Zhang and J. Chen, *Energy Environ. Sci.*, 2022, **15**, 1711–1759.
55 J. Liu, B. Yuan, N. He, L. Dong, D. Chen, S. Zhong, Y. Ji, J. Han, C. Yang, Y. Liu and W. He, *Energy Environ. Sci.*, 2023, **16**, 1024–1034.
56 X. Dong, Y. Lin, P. Li, Y. Ma, J. Huang, D. Bin, Y. Wang, Y. Qi and Y. Xia, *Angew. Chem., Int. Ed.*, 2019, **58**, 5623–5627.
57 P. Lai, B. Huang, X. Deng, J. Li, H. Hua, P. Zhang and J. Zhao, *Chem. Eng. J.*, 2023, **461**, 141904.
58 S. Weng, X. Zhang, G. Yang, S. Zhang, B. Ma, Q. Liu, Y. Liu, C. Peng, H. Chen, H. Yu, X. Fan, T. Cheng, L. Chen, Y. Li, Z. Wang and X. Wang, *Nat. Commun.*, 2023, **14**, 4474.
59 J. Holoubek, M. Yu, S. Yu, M. Li, Z. Wu, D. Xia, P. Bhaladhare, M. S. Gonzalez, T. A. Pascal and Z. Chen, *ACS Energy Lett.*, 2020, **5**, 1438–1447.
60 G. Cai, H. Gao, M. Li, V. Gupta, J. Holoubek, T. A. Pascal, P. Liu and Z. Chen, *Angew. Chem., Int. Ed.*, 2024, **63**, e202316786.
61 C. Chen, S. Zhang, C. Xu, J. Yang, Y. Hu, L. Yu, P. Li, B. Qu and M. Wu, *J. Energy Chem.*, 2025, **101**, 608–618.
62 S. He, H. Yuan, P. Zhu, X. Wang and B. Xu, *Chem. Eng. J.*, 2024, **500**, 156302.
63 F. Hai, Y. Yi, J. Guo, X. Gao, W. Chen, X. Tian, W. Tang and M. Li, *Chem. Eng. J.*, 2023, **472**, 144993.
64 M. Mao, X. Ji, Q. Wang, Z. Lin, M. Li, T. Liu, C. Wang, Y.-S. Hu, H. Li, X. Huang, L. Chen and L. Suo, *Nat. Commun.*, 2023, **14**, 1082.
65 T. Yang, S. Li, W. Wang, J. Lu, W. Fan, X. Zuo and J. Nan, *J. Power Sources*, 2021, **505**, 230055.
66 X. Li, F. Luo, M. Yu, R. Liu, S. Zhao and S. Fang, *Energy Storage Mater.*, 2025, **75**, 104048.
67 Y. Chen, Z. Ma, Y. Wang, P. Kumar, F. Zhao, T. Cai, Z. Cao, L. Cavallo, H. Cheng, Q. Li and J. Ming, *Energy Environ. Sci.*, 2024, **17**, 5613–5626.
68 Y. Zhang, F. Li, Y. Cao, M. Yang, X. Han, Y. Ji, K. Chen, L. Liang, J. Sun and G. Hou, *Adv. Funct. Mater.*, 2024, **34**, 2315527.
69 Y. Meng, D. Zhou, R. Liu, Y. Tian, Y. Gao, Y. Wang, B. Sun, F. Kang, M. Armand, B. Li, G. Wang and D. Aurbach, *Nat. Energy*, 2023, **8**, 1023–1033.
70 C. Yan, Y.-X. Yao, X. Chen, X.-B. Cheng, X.-Q. Zhang, J.-Q. Huang and Q. Zhang, *Angew. Chem., Int. Ed.*, 2018, **57**, 14055–14059.
71 S. Stuckenberg, M. M. Bela, C.-T. Lechtenfeld, M. Mense, V. Küpers, T. T. K. Ingber, M. Winter and M. C. Stan, *Small*, 2024, **20**, 2305203.
72 C.-B. Jin, N. Yao, Y. Xiao, J. Xie, Z. Li, X. Chen, B.-Q. Li, X.-Q. Zhang, J.-Q. Huang and Q. Zhang, *Adv. Mater.*, 2023, **35**, 2208340.
73 S. C. Kim, X. Gao, S.-L. Liao, H. Su, Y. Chen, W. Zhang, L. C. Greenburg, J.-A. Pan, X. Zheng, Y. Ye, M. S. Kim, P. Sayavong, A. Brest, J. Qin, Z. Bao and Y. Cui, *Nat. Commun.*, 2024, **15**, 1268.
74 J. Xiang and Y.-C. Lu, *ACS Nano*, 2024, **18**, 10726–10737.
75 Z. Zhao, A. Wang, A. Chen, Y. Zhao, Z. Hu, K. Wu and J. Luo, *Angew. Chem., Int. Ed.*, 2024, **63**, e202412239.
76 Y. M. Kim, B. K. Park, S. Kang, S. J. Yang, S. H. Choi, D.-J. Yoo and K. J. Kim, *Adv. Funct. Mater.*, 2024, **34**, 2408365.
77 X. Peng, T. Wang, B. Liu, Y. Li and T. Zhao, *Energy Environ. Sci.*, 2022, **15**, 5350–5361.
78 J. Zou, H. Yang, S. Wu, Z. Xiao, Z. Jiang, W. Shen and Y. Li, *J. Colloid Interface Sci.*, 2025, **683**, 281–290.
79 X. Zhu, J. Chen, G. Liu, Y. Mo, Y. Xie, K. Zhou, Y. Wang and X. Dong, *Angew. Chem., Int. Ed.*, 2025, **64**, e202412859.
80 Y. Lin, Z. Yang, X. Zhang, Y. Liu, G. Hu, S. Chen and Y. Zhang, *Energy Storage Mater.*, 2023, **58**, 184–194.
81 R. Xu, J.-F. Ding, X.-X. Ma, C. Yan, Y.-X. Yao and J.-Q. Huang, *Adv. Mater.*, 2021, **33**, 2105962.
82 X. Li, M. Li, Y. Liu, Y. Jie, W. Li, Y. Chen, F. Huang, Y. Zhang, T. M. Sohail, S. Wang, X. Zhu, T. Cheng, M. D. Gu, S. Jiao and R. Cao, *J. Am. Chem. Soc.*, 2024, **146**, 17023–17031.
83 L. Chen, Q. Zhang, C. Song, Y. Jiang, X. Sheng, H. Pan, L. Yang, S. Wu, L. Zeng, D. Sun, C. Wang, T. Wang, Y. Li and T. Zhao, *Angew. Chem., Int. Ed.*, 2025, **64**, e202422791.
84 J. Zhang, Q. Li, Y. Zeng, Z. Tang, D. Sun, D. Huang, Y. Tang and H. Wang, *ACS Energy Lett.*, 2023, **8**, 1752–1761.
85 Z. Wang, X. Che, D. Wang, Y. Wang, X. He, Y. Zhu and B. Zhang, *Angew. Chem., Int. Ed.*, 2024, **63**, e202404109.
86 Y. Yang, X. Wang, J. Zhu, L. Tan, N. Li, Y. Chen, L. Wang, Z. Liu, X. Yao, X. Wang, X. Ji and Y. Zhu, *Angew. Chem., Int. Ed.*, 2024, **63**, e202409193.
87 Z. Wang, X. Che, D. Wang, Y. Wang, X. He, Y. Zhu and B. Zhang, *J. Mater. Chem. A*, 2022, **10**, 12035–12046.
88 Y. Liao, M. Zhou, L. Yuan, K. Huang, D. Wang, Y. Han, J. Meng, Y. Zhang, Z. Li and Y. Huang, *Adv. Energy Mater.*, 2023, **13**, 2301477.
89 Z. Li, Y. Liao, H. Ji, X. Lin, Y. Wei, S. Hao, X. Hu, L. Yuan, Z. Huang and Y. Huang, *Adv. Energy Mater.*, 2025, **15**, 2404120.
90 Y. Yang, Q. Li, H. Li, J. Ruan, F. Wang, Z. Li, J. Yang, J. Zhang, U. Çağlayan, D. Sun, F. Fang, M. Kunduraci and F. Wang, *Angew. Chem., Int. Ed.*, 2025, **64**, e202419653.
91 Y. Zhao, T. Zhou, D. Baster, M. E. Kazzi, J. W. Choi and A. Coskun, *ACS Energy Lett.*, 2023, **8**, 3180–3187.
92 T. Zhou, Y. Zhao, M. E. Kazzi, J. W. Choi and A. Coskun, *Angew. Chem., Int. Ed.*, 2022, **61**, e202115884.
93 Y. Zhao, T. Zhou, T. Ashirov, M. E. Kazzi, C. Cancellieri, L. P. H. Jeurgens, J. W. Choi and A. Coskun, *Nat. Commun.*, 2022, **13**, 2575.
94 Y. Zhao, T. Zhou, M. E. Kazzi and A. Coskun, *ACS Appl. Energy Mater.*, 2022, **5**, 7784–7790.

95 K. Lee, S.-H. Kwon, J. Kim, E. Park, I. Kim, H. C. Ahn, A. Coskun and J. W. Choi, *ACS Energy Lett.*, 2024, **9**, 2201–2211.
96 M. Wu, Z. Wang, W. Zhang, C. Jayawardana, Y. Li, F. Chen, B. Nan, B. L. Lucht and C. Wang, *Angew. Chem., Int. Ed.*, 2023, **62**, e202216169.
97 G.-X. Li, V. Koverga, A. Nguyen, R. Kou, M. Ncube, H. Jiang, K. Wang, M. Liao, H. Guo, J. Chen, N. Dandu, A. T. Ngo and D. Wang, *Nat. Energy*, 2024, **9**, 817–827.
98 M. Li, C. Wang, K. Davey, J. Li, G. Li, S. Zhang, J. Mao and Z. Guo, *SmartMat*, 2023, **4**, e1185.
99 S. Chen, J. Fan, Z. Cui, L. Tan, D. Ruan, X. Zhao, J. Jiang, S. Jiao and X. Ren, *Angew. Chem., Int. Ed.*, 2023, **62**, e202219310.
100 S. Chen, J. Zheng, D. Mei, K. S. Han, M. H. Engelhard, W. Zhao, W. Xu, J. Liu and J.-G. Zhang, *Adv. Mater.*, 2018, **30**, 1706102.
101 H. Wang, Z. Yu, X. Kong, S. C. Kim, D. T. Boyle, J. Qin, Z. Bao and Y. Cui, *Joule*, 2022, **6**, 588–616.
102 Y. Chen, S.-L. Liao, H. Gong, Z. Zhang, Z. Huang, S. C. Kim, E. Zhang, H. Lyu, W. Yu, Y. Lin, P. Sayavong, Y. Cui, J. Qin and Z. Bao, *Chem. Sci.*, 2024, **15**, 19805–19819.
103 T. Ma, Y. Ni, Q. Wang, W. Zhang, S. Jin, S. Zheng, X. Yang, Y. Hou, Z. Tao and J. Chen, *Angew. Chem., Int. Ed.*, 2022, **61**, e202207927.
104 K. Ding, C. Xu, Z. Peng, X. Long, J. Shi, Z. Li, Y. Zhang, J. Lai, L. Chen, Y.-P. Cai and Q. Zheng, *ACS Appl. Mater. Interfaces*, 2022, **14**, 44470–44478.
105 Y. Chen, Z. Yu, P. Rudnicki, H. Gong, Z. Huang, S. C. Kim, J.-C. Kim, X. Kong, J. Qin, Y. Cui and Z. Bao, *J. Am. Chem. Soc.*, 2021, **143**, 18703–18713.
106 T. D. Pham and K.-K. Lee, *Small*, 2021, **17**, 2100133.
107 Z. Wang, C. Chen, D. Wang, Y. Zhu and B. Zhang, *Angew. Chem., Int. Ed.*, 2023, **62**, e202303950.
108 E. Park, J. Park, K. Lee, Y. Zhao, T. Zhou, G. Park, M.-G. Jeong, M. Choi, D.-J. Yoo, H.-G. Jung, A. Coskun and J. W. Choi, *ACS Energy Lett.*, 2023, **8**, 179–188.
109 A.-M. Li, O. Borodin, T. P. Pollard, W. Zhang, N. Zhang, S. Tan, F. Chen, C. Jayawardana, B. L. Lucht, E. Hu, X.-Q. Yang and C. Wang, *Nat. Chem.*, 2024, **16**, 922–929.
110 P. Ma, U. Le, K.-H. Wang, M. C. Vu, P. Mirmira and C. V. Amanchukwu, *J. Electrochem. Soc.*, 2024, **171**, 120536.
111 Y. Liu, Y. Lin, Z. Yang, C. Lin, X. Zhang, S. Chen, G. Hu, B. Sa, Y. Chen and Y. Zhang, *ACS Nano*, 2023, **17**, 19625–19639.
112 S. Chen, W. Zhu, L. Tan, D. Ruan, J. Fan, Y. Chen, X. Meng, Q. Nian, X. Zhao, J. Jiang, Z. Wang, S. Jiao, X. Wu and X. Ren, *ACS Appl. Mater. Interfaces*, 2023, **15**, 13155–13164.
113 A. Dutta, K. Matsushita and Y. Kubo, *Adv. Sci.*, 2024, **11**, 2404245.
114 J. Wu, Z. Gao, Y. Tian, Y. Zhao, Y. Lin, K. Wang, H. Guo, Y. Pan, X. Wang, F. Kang, N. Tavajohi, X. Fan and B. Li, *Adv. Mater.*, 2023, **35**, 2303347.
115 X. Li, Y. Pan, Y. Liu, Y. Jie, S. Chen, S. Wang, Z. He, X. Ren, T. Cheng, R. Cao and S. Jiao, *Carbon Neutrality*, 2023, **2**, 34.
116 J. Holoubek, H. Liu, Z. Wu, Y. Yin, X. Xing, G. Cai, S. Yu, H. Zhou, T. A. Pascal, Z. Chen and P. Liu, *Nat. Energy*, 2021, **6**, 303–313.
117 Z. Li, H. Rao, R. Atwi, B. M. Sivakumar, B. Gwalani, S. Gray, K. S. Han, T. A. Everett, T. A. Ajantiwalay, V. Murugesan, N. N. Rajput and V. G. Pol, *Nat. Commun.*, 2023, **14**, 868.
118 G. Cai, J. Holoubek, M. Li and Z. Chen, *Proc. Natl. Acad. Sci. U. S. A.*, 2022, **119**, e2200392119.
119 H. Li, Y. Kang, W. Wei, C. Yan, X. Ma, H. Chen, Y. Sang, H. Liu and S. Wang, *Nano-Micro Lett.*, 2024, **16**, 197.
120 R. Qiao, Y. Zhao, S. Zhou, H. Zhang, F. Liu, T. Zhou, B. Sun, H. Fan, C. Li, Y. Zhang, F. Liu, X. Ding, J. W. Choi, A. Coskun and J. Song, *Chem*, 2025, **11**, 102306.
121 H. Zhang, Z. Zeng, F. Ma, Q. Wu, X. Wang, S. Cheng and J. Xie, *Angew. Chem., Int. Ed.*, 2023, **62**, e202300771.
122 Z. He, Y. Chen, F. Huang, Y. Jie, X. Li, R. Cao and S. Jiao, *Acta Phys. – Chim. Sin.*, 2022, **38**, 2205005.
123 N. von Aspern, G.-V. Röschenthaler, M. Winter and I. Cekic-Laskovic, *Angew. Chem., Int. Ed.*, 2019, **58**, 15978–16000.
124 S. C. Kim, X. Kong, R. A. Vilá, W. Huang, Y. Chen, D. T. Boyle, Z. Yu, H. Wang, Z. Bao, J. Qin and Y. Cui, *J. Am. Chem. Soc.*, 2021, **143**, 10301–10308.
125 Z. Zhang, Y. Li, R. Xu, W. Zhou, Y. Li, S. T. Oyakhire, Y. Wu, J. Xu, H. Wang, Z. Yu, D. T. Boyle, W. Huang, Y. Ye, H. Chen, J. Wan, Z. Bao, W. Chiu and Y. Cui, *Science*, 2022, **375**, 66–70.
126 T. Jang, S. Y. Cho, J. Kim, E. Choi, S. L. Holzmann, U. Krewer, H. Shin and H. R. Byon, *Small*, 2025, **21**, 2500166.
127 A. A. Hizbullin, I. V. Kutovaya, G. A. Kirakosyan, D. A. Cheshkov, D. N. Govorov, D. A. Aksyonov, V. A. Nikitina, S. S. Fedotov and O. I. Shmatova, *J. Power Sources*, 2025, **630**, 236086.
128 Y. Zhao, T. Zhou, M. Mensi, J. W. Choi and A. Coskun, *Nat. Commun.*, 2023, **14**, 299.
129 Z. Yu, P. E. Rudnicki, Z. Zhang, Z. Huang, H. Celik, S. T. Oyakhire, Y. Chen, X. Kong, S. C. Kim, X. Xiao, H. Wang, Y. Zheng, G. A. Kamat, M. S. Kim, S. F. Bent, J. Qin, Y. Cui and Z. Bao, *Nat. Energy*, 2022, **7**, 94–106.
130 C.-C. Su, J. Shi, R. Amine, M. He, S.-B. Son, J. Guo, M. Jiang and K. Amine, *Nano Energy*, 2023, **110**, 108335.
131 P. Ma, P. Mirmira and C. V. Amanchukwu, *ACS Cent. Sci.*, 2021, **7**, 1232–1244.
132 I. R. Choi, Y. Chen, A. Shah, J. Florian, C. Serrao, J. Holoubek, H. Lyu, E. Zhang, J. H. Lee, Y. Lin, S. C. Kim, H. Park, P. Zhang, J. Lee, J. Qin, Y. Cui and Z. Bao, *Nat. Energy*, 2025, **10**, 365–379.
133 L.-Q. Wu, Z. Li, Z.-Y. Fan, K. Li, J. Li, D. Huang, A. Li, Y. Yang, W. Xie and Q. Zhao, *J. Am. Chem. Soc.*, 2024, **146**, 5964–5976.
134 J. Chen, H. Lu, X. Kong, J. Liu, J. Liu, J. Yang, Y. Nuli and J. Wang, *Angew. Chem., Int. Ed.*, 2024, **63**, e202317923.

135 X. Yuan, X. Chen, Y. Zhou, Z. Yu and X. Kong, *J. Energy Chem.*, 2025, **102**, 52–62.
136 D. Ruan, L. Tan, S. Chen, J. Fan, Q. Nian, L. Chen, Z. Wang and X. Ren, *JACS Au*, 2023, **3**, 953–963.
137 Y. Xue, Y. Wang, H. Zhang, W. Kong, Y. Zhou, B. Kang, Z. Huang and H. Xiang, *Angew. Chem., Int. Ed.*, 2025, **64**, e202414201.
138 E. Zhang, Y. Chen, J. Holoubek and Z. Bao, *Proc. Natl. Acad. Sci. U. S. A.*, 2025, **122**, e2418623122.
139 G. Zhang, J. Chang, L. Wang, J. Li, C. Wang, R. Wang, G. Shi, K. Yu, W. Huang, H. Zheng, T. Wu, Y. Deng and J. Lu, *Nat. Commun.*, 2023, **14**, 1081.
140 Z. Li, J. Zhang, W. Xie and Q. Zhao, *Int. J. Quantum Chem.*, 2024, **124**, e27515.
141 L. Tan, S. Chen, Y. Chen, J. Fan, D. Ruan, Q. Nian, L. Chen, S. Jiao and X. Ren, *Angew. Chem., Int. Ed.*, 2022, **61**, e202203693.
142 M. Fang, B. Du, X. Zhang, X. Dong, X. Yue and Z. Liang, *Angew. Chem., Int. Ed.*, 2024, **63**, e202316839.
143 G.-X. Li, X. Lyu, A. Nguyen, R. Kou, C. George, S. Wu, R. Li, K. Wang, T. Li and D. Wang, *Adv. Energy Mater.*, 2025, **15**, 2405680.
144 J. Shi, C. Xu, J. Lai, Z. Li, Y. Zhang, Y. Liu, K. Ding, Y.-P. Cai, R. Shang and Q. Zheng, *Angew. Chem., Int. Ed.*, 2023, **62**, e202218151.
145 H. Wang, Z. Yu, X. Kong, W. Huang, Z. Zhang, D. G. Mackanic, X. Huang, J. Qin, Z. Bao and Y. Cui, *Adv. Mater.*, 2021, **33**, 2008619.
146 J. Zhang, H. Zhang, R. Li, L. Lv, D. Lu, S. Zhang, X. Xiao, S. Geng, F. Wang, T. Deng, L. Chen and X. Fan, *J. Energy Chem.*, 2023, **78**, 71–79.
147 Y. Yamada, K. Furukawa, K. Sodeyama, K. Kikuchi, M. Yaegashi, Y. Tateyama and A. Yamada, *J. Am. Chem. Soc.*, 2014, **136**, 5039–5046.
148 S. H. Lee, J.-Y. Hwang, S.-J. Park, G.-T. Park and Y.-K. Sun, *Adv. Funct. Mater.*, 2019, **29**, 1902496.
149 P. Xiao, X. Yun, Y. Chen, X. Guo, P. Gao, G. Zhou and C. Zheng, *Chem. Soc. Rev.*, 2023, **52**, 5255–5316.
150 D. Lu, R. Li, M. M. Rahman, P. Yu, L. Lv, S. Yang, Y. Huang, C. Sun, S. Zhang, H. Zhang, J. Zhang, X. Xiao, T. Deng, L. Fan, L. Chen, J. Wang, E. Hu, C. Wang and X. Fan, *Nature*, 2024, **627**, 101–107.
151 L. Luo, K. Chen, H. Chen, H. Li, R. Cao, X. Feng, W. Chen, Y. Fang and Y. Cao, *Adv. Mater.*, 2024, **36**, 2308881.
152 Z. Wang, Y. Wang, Y. Xin, Q. Zhou, X. Ding, L. Liu, T. Song, F. Wu, Z. Wei and H. Gao, *Chem. Sci.*, 2024, **15**, 16669–16680.
153 F. Zhang, P. Zhang, W. Zhang, P. R. Gonzalez, D. Q. Tan and Y. Ein-Eli, *Adv. Mater.*, 2024, **36**, 2410277.
154 M. Li, Y. Liu, X. Yang, Q. Zhang, Y. Cheng, L. Deng, Q. Zhou, T. Cheng and M. D. Gu, *Adv. Mater.*, 2024, **36**, 2404271.
155 Z. Peng, X. Cao, P. Gao, H. Jia, X. Ren, S. Roy, Z. Li, Y. Zhu, W. Xie, D. Liu, Q. Li, D. Wang, W. Xu and J.-G. Zhang, *Adv. Funct. Mater.*, 2020, **30**, 2001285.
156 H. Moon, S.-J. Cho, D.-E. Yu and S.-Y. Lee, *Energy Environ. Mater.*, 2023, **6**, e12383.
157 T. Qin, H. Yang, L. Wang, W. Xue, N. Yao, Q. Li, X. Chen, X. Yang, X. Yu, Q. Zhang and H. Li, *Angew. Chem., Int. Ed.*, 2024, **63**, e202408902.
158 M. Mao, L. Gong, X. Wang and C. Wang, *Proc. Natl. Acad. Sci. U. S. A.*, 2024, **121**, e2316212121.
159 J. Lian, S. Tan, J. Lou, J. Lan, W. Cui, Z. Han, G. Zheng, T. Hou, W. Lv, M. Liu and Z. Wang, *Adv. Funct. Mater.*, 2025, **35**, 2421802.
160 X. Zhou, M. Kozdra, Q. Ran, K. Deng, H. Zhou, D. Brandell and J. Wang, *Nanoscale*, 2022, **14**, 17237–17246.
161 Q.-K. Zhang, X.-Q. Zhang, L.-P. Hou, S.-Y. Sun, Y.-X. Zhan, J.-L. Liang, F.-S. Zhang, X.-N. Feng, B.-Q. Li and J.-Q. Huang, *Adv. Energy Mater.*, 2022, **12**, 2200139.
162 W. Wu, Y. Bo, D. Li, Y. Liang, J. Zhang, M. Cao, R. Guo, Z. Zhu, L. Ci, M. Li and J. Zhang, *Nano-Micro Lett.*, 2022, **14**, 44.
163 Q. Wang, Z. Yao, C. Zhao, T. Verhallen, D. P. Tabor, M. Liu, F. Ooms, F. Kang, A. Aspuru-Guzik, Y.-S. Hu, M. Wagemaker and B. Li, *Nat. Commun.*, 2020, **11**, 4188.
164 Y. Yang, S. Ma, H. Yin, Y. Li, S. Chen, Y. Zhang, D. Li, F. Dong, Y. Zhang, H. Xie and L. Cong, *Adv. Sci.*, 2024, **11**, 2404248.
165 Y. Wu, Q. Zhang, N. Wang and K. Deng, *Energy Storage Mater.*, 2025, **75**, 104066.
166 Y. Gao, L. Zhu, B. Wang, Y. Xu, J. Chai, A. Fu, H. Li, J. Li, Y. Peng, Y. Zheng, Y. Wang, J. Y. Lee, D. Lv and Z. Liu, *ACS Energy Lett.*, 2024, **9**, 3931–3938.
167 M. Fang, X. Yue, Y. Dong, Y. Chen and Z. Liang, *Joule*, 2024, **8**, 91–103.
168 W. Hou, P. Zhou, H. Gu, Y. Ou, Y. Xia, X. Song, Y. Lu, S. Yan, Q. Cao, H. Liu, F. Liu and K. Liu, *ACS Nano*, 2023, **17**, 17527–17535.
169 S. Gu, Y. Zhang, M. Li, Q. Lin, G. Xu and N. Zhang, *Angew. Chem., Int. Ed.*, 2025, **64**, e202410020.
170 Y. Shuai, Y. Hu, X. Gong, Z. Xu, L. Li, L. Zhang, M. Li, J. Zhou and M. Li, *Chem. Eng. J.*, 2025, **505**, 159101.
171 Y. Li, X. Hao, H. Liu, J. Zou and W. Wang, *ACS Appl. Mater. Interfaces*, 2024, **16**, 55362–55371.
172 S. Ko, Y. Yamada and A. Yamada, *Joule*, 2021, **5**, 998–1009.
173 X. Ren, S. Chen, H. Lee, D. Mei, M. H. Engelhard, S. D. Burton, W. Zhao, J. Zheng, Q. Li, M. S. Ding, M. Schroeder, J. Alvarado, K. Xu, Y. S. Meng, J. Liu, J.-G. Zhang and W. Xu, *Chem*, 2018, **4**, 1877–1892.
174 X. Fan and C. Wang, *Chem. Soc. Rev.*, 2021, **50**, 10486–10566.
175 J. Fu, X. Ji, J. Chen, L. Chen, X. Fan, D. Mu and C. Wang, *Angew. Chem., Int. Ed.*, 2020, **59**, 22194–22201.
176 B.-H. Zhang, P.-P. Chen, Y.-L. Hou, J.-Z. Chen, H.-Y. Wang, W.-X. Wen, Z.-A. Li, J.-T. Lei and D.-L. Zhao, *Small*, 2024, **20**, 2402123.
177 J. Zhou, B. Ma, Q. Wang, L. Su, K. Yang, X. Song, X. Dou, M. Wang, X. Shangguan and F. Li, *Chem. Eng. J.*, 2025, **504**, 158857.

178 J. Zhou, C. Zhang, H. Wang, Y. Guo, C. Xie, Y. Luo, C. Wang, S. Wen, J. Cai, W. Yu, F. Chen, Y. Zhang, Q. Huang and Z. Zheng, *Adv. Sci.*, 2024, **11**, 2410129.
179 T. Zhou, C. Lei, J. Li, H. Wang, T. Liu, X. He and X. Liang, *Angew. Chem., Int. Ed.*, 2024, **63**, e202408728.
180 P. Ding, H. Yuan, L. Xu, L. Wu, H. Du, S. Zhao, D. Yu, Z. Qin, H. Liu, Y. Li, X. Zhang, H. Yu, M. Tang, Y. Ren, L. Li and C.-W. Nan, *Adv. Mater.*, 2025, **37**, 24131654.
181 Z. Li, L. Wang, X. Huang and X. He, *Adv. Funct. Mater.*, 2024, **34**, 2408319.
182 W. Xue, Z. Shi, M. Huang, S. Feng, C. Wang, F. Wang, J. Lopez, B. Qiao, G. Xu, W. Zhang, Y. Dong, R. Gao, Y. Shao-Horn, J. A. Johnson and J. Li, *Energy Environ. Sci.*, 2020, **13**, 212–220.
183 W. Xue, M. Huang, Y. Li, Y. G. Zhu, R. Gao, X. Xiao, W. Zhang, S. Li, G. Xu, Y. Yu, P. Li, J. Lopez, D. Yu, Y. Dong, W. Fan, Z. Shi, R. Xiong, C.-J. Sun, I. Hwang, W.-K. Lee, Y. Shao-Horn, J. A. Johnson and J. Li, *Nat. Energy*, 2021, **6**, 495–505.
184 W. Xue, R. Gao, Z. Shi, X. Xiao, W. Zhang, Y. Zhang, Y. G. Zhu, I. Waluyo, Y. Li, M. R. Hill, Z. Zhu, S. Li, O. Kuznetsov, Y. Zhang, W.-K. Lee, A. Hunt, A. Harutyunyan, Y. Shao-Horn, J. A. Johnson and J. Li, *Energy Environ. Sci.*, 2021, **14**, 6030–6040.
185 G. Zhang, J. Li, Q. Wang, H. Wang, J. Wang, K. Yu, J. Chang, C. Wang, X. Hong, Q. Ma and Y. Deng, *ACS Energy Lett.*, 2023, **8**, 2868–2877.
186 S. Kim, J. H. Jeon, K. Park, S. H. Kweon, J.-H. Hyun, C. Song, D. Lee, G. Song, S.-H. Yu, T. K. Lee, S. K. Kwak, K. T. Lee, S. Y. Hong and N.-S. Choi, *Adv. Mater.*, 2024, **36**, 2401615.
187 C. Sun, R. Li, S. Weng, C. Zhu, L. Chen, S. Jiang, L. Li, X. Xiao, C. Liu, L. Chen, T. Deng, X. Wang and X. Fan, *Angew. Chem., Int. Ed.*, 2024, **63**, e202400761.
188 L. Pompizii, M. Liu, L. Braks, T. Ashirov, T. Zhou, M. Mensi, D. Park, J. W. Choi and A. Coskun, *ACS Energy Lett.*, 2025, **10**, 246–253.
189 Y. Wang, Y. Zhao, S. Zhang, L. Shang, Y. Ni, Y. Lu, Y. Li, Z. Yan, Z. Miao and J. Chen, *Angew. Chem., Int. Ed.*, 2024, **63**, e202412108.
190 H. Sun, J. Liu, J. He, H. Wang, G. Jiang, S. Qi and J. Ma, *Sci. Bull.*, 2022, **67**, 725–732.
191 S. Zhang, S. Li and Y. Lu, *eScience*, 2021, **1**, 163–177.
192 M. Liu, X. Li, B. Zhai, Z. Zeng, W. Hu, S. Lei, H. Zhang, S. Cheng and J. Xie, *Batteries Supercaps*, 2022, **5**, e202100407.
193 C. Liao, L. Han, W. Wang, W. Li, X. Mu, Y. Kan, J. Zhu, Z. Gui, X. He, L. Song and Y. Hu, *Adv. Funct. Mater.*, 2023, **33**, 2212605.
194 Q. Guo, R. Luo, Z. Tang, X. Li, X. Feng, Z. Ding, B. Gao, X. Zhang, K. Huo and Y. Zheng, *ACS Nano*, 2023, **17**, 24227–24241.
195 Z. Ni, C. Wei, Z. Wang, Y. Li, X. Zhang, S. Xiong and J. Feng, *Energy Storage Mater.*, 2024, **71**, 103603.
196 Y. Wang, C. Zheng, W. Xie, X. Liu, Y. Lu, Y. Hou, T. Ma, Z. Yan and J. Chen, *Adv. Mater.*, 2024, **36**, 2312302.
197 S. Wu, X. Liu, Z. Hao, X. Sun, J. Hou, L. Shang, L. Wang, K. Zhang, H. Li, Z. Yan and J. Chen, *J. Am. Chem. Soc.*, 2024, **146**, 28770–28782.
198 Q. Zheng, Y. Yamada, R. Shang, S. Ko, Y.-Y. Lee, K. Kim, E. Nakamura and A. Yamada, *Nat. Energy*, 2020, **5**, 291–298.
199 Z. Xu, X. Zhang, J. Yang, X. Cui, Y. Nuli and J. Wang, *Nat. Commun.*, 2024, **15**, 9856.
200 Y. Huang, R. Li, S. Weng, H. Zhang, C. Zhu, D. Lu, C. Sun, X. Huang, T. Deng, L. Fan, L. Chen, X. Wang and X. Fan, *Energy Environ. Sci.*, 2022, **15**, 4349–4361.
201 X. Yin, B. Li, H. Liu, B. Wen, J. Liu, M. Bai, Y. Zhang, Y. Zhao, X. Cui, Y. Su, G. Gao, S. Ding and W. Yu, *Joule*, 2025, **9**, 101823.
202 G. Huang, Y. Liao, H. Liu, X. Jin, M. Guan, F. Yu, B. Dai and Y. Li, *ACS Nano*, 2024, **18**, 15802–15814.
203 S. Li, Y. Ma, L. Zheng, M. Li, C. Ma, H. Yu, X. Niu and L. Wang, *Energy Storage Mater.*, 2025, **76**, 104124.
204 Z. Piao, X. Wu, H.-R. Ren, G. Lu, R. Gao, G. Zhou and H.-M. Cheng, *J. Am. Chem. Soc.*, 2023, **145**, 24260–24271.
205 Y. Li, M. Liu, K. Wang, C. Li, Y. Lu, A. Choudhary, T. Ottley, D. Bedrov, L. Xing and W. Li, *Adv. Energy Mater.*, 2023, **13**, 2300918.
206 C. Sun, R. Li, C. Zhu, L. Chen, S. Weng, C. Liu, T. Deng, L. Chen, X. Wang and X. Fan, *ACS Energy Lett.*, 2023, **8**, 4119–4128.
207 Y. Wang, Y. Ni, S. Xu, Y. Lu, L. Shang, Z. Yang, K. Zhang, Z. Yan, W. Xie and J. Chen, *J. Am. Chem. Soc.*, 2025, **147**, 10772–10783.
208 B. Ma, H. Zhang, R. Li, S. Zhang, L. Chen, T. Zhou, J. Wang, R. Zhang, S. Ding, X. Xiao, T. Deng, L. Chen and X. Fan, *Nat. Chem.*, 2024, **16**, 1427–1435.
209 Y. Wu, Z. Zeng, H. Zhang, M. Liu, S. Lei, W. Zhong, S. Cheng and J. Xie, *Energy Storage Mater.*, 2024, **70**, 103499.
210 S. Ko, T. Obukata, T. Shimada, N. Takenaka, M. Nakayama, A. Yamada and Y. Yamada, *Nat. Energy*, 2022, **7**, 1217–1224.
211 S. Zhang, R. Li, T. Deng, Q. Ma, X. Hong, H. Zhang, R. Zhang, S. Ding, Y. Wu, H. Zhu, M. Li, H. Zhang, D. Lu, B. Ma, L. Lv, Y. Li, L. Chen, Y. Shen, R. Guo and X. Fan, *Nat. Energy*, 2024, **9**, 1285–1296.
212 Y. Yang, N. Yao, Y.-C. Gao, X. Chen, Y.-X. Huang, S. Zhang, H.-B. Zhu, L. Xu, Y.-X. Yao, S.-J. Yang, Z. Liao, Z. Li, X.-F. Wen, P. Wu, T.-L. Song, J.-H. Yao, J.-K. Hu, C. Yan, J.-Q. Huang and Q. Zhang, *Angew. Chem., Int. Ed.*, 2025, **64**, e202505212.
213 Q. Jia, H. Liu, X. Wang, Q. Tao, L. Zheng, J. Li, W. Wang, Z. Liu, X. Gu, T. Shen, S. Hou, Z. Jin and J. Ma, *Angew. Chem., Int. Ed.*, 2025, **64**, e202424493.